

Re-interpretation of structure-function correlations and inhibitions of mammalian cyclooxygenase isozymes with murburn concept

Daniel Andrew Gideon^{1}, Pushparaj Annadurai², Abhinav Parashar³, Kelath Murali Manoj^{4,5*}*

*Corresponding authors

¹*Department of Biochemistry, St. Joseph's University,
Langford Road, Bengaluru, Karnataka, India-560027.
daniel.gideon@sju.edu.in (ORCID: 0000-0003-2470-550X)

² Nandha Siddha Medical College and Hospital, Erode, Tamil Nadu, India-638052.
pushpasaya10@gmail.com (ORCID: 0000-0002-6215-7172)

³ Department of Biological Sciences, P. D. Patel Institute of Applied Sciences, Charotar University of Science and Technology, Changa, Anand, Gujarat, India-388421.
abhinavparashar.as@charusat.ac.in
(ORCID: 0000-0003-4229-0248)

Corresponding author:

⁴*Satyamjayatu: The Science & Ethics Foundation,
Kulappully, Shoranur-2, Palakkad District, Kerala, India-679122.
murman@satyamjayatu.com (ORCID: 0000-0003-4515-994X)

⁵*Biomedical ScDivision, School of Artificial Intelligence,
Amrita Vishwa Vidyapeetham (Amrita University - Coimbatore Campus),
Amritanagar, Ettimadai, Coimbatore, Tamil Nadu, India-641112.

Number of figures: 8

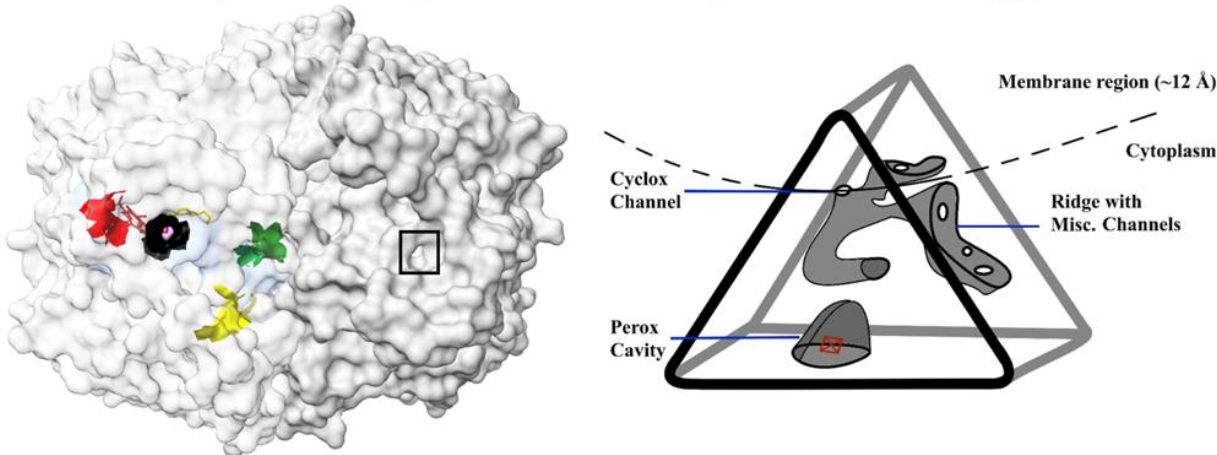
Number of tables: 4

Keywords: cyclooxygenase, inflammation, murburn concept, prostaglandins, murzyme, diffusible reactive species (DRS)

Abstract: As per the acclaimed classical mechanism, cyclooxygenase (COX) supposedly has two functional sites: an aqueous phase exposed peroxidase (perox) site and a lipid-phase buried cyclooxygenase (cyclox) site. Peroxidative reaction of heme-Fe at perox site forms a high-potential Compound I species, which supposedly generates a tyrosine radical within the cyclox site via an electron-tunneling mechanism. Thereafter, two molecules of triplet oxygen are purportedly inserted into the bound lipid substrate at cyclox site to yield PGG₂. Subsequently, PGG₂ is moved to perox site where it is converted to PGH₂. Herein, we surveyed diverse COX proteins and tested out *in silico* binding interactions with various substrates and inhibitors. We found that our ligand-docking results and significant experimental reports in literature support a DRS (diffusible reactive species)-based murburn mechanism, wherein the actual “oxygen-insertion reaction step” may occur beyond the physical constraints of the deep-seated active-site (wherein Fe-O or TyrO species directly interact with the substrates’ C-atom). Further, our interpretations are also supported by the earlier reports that question the wisdom of using “induced fit” type mechanism for fitting the protein’s crystal-structure, by invoking extensive “conformation-change” based explanations.

Graphical/Text Highlight

Cyclooxygenase is a murzyme! *Implication of murburn concept in immunology*



Cyclooxygenase shows multiple channels for diffusible reactive species traffic!

1. Introduction

Cyclooxygenase (COX) is a membrane-embedded heme-protein that plays crucial roles in diverse tissues and scenarios- eg. inflammation, immune response and cancer. The enzyme activity inserts two molecules of oxygen into an unsaturated long-chain substrate like arachidonic acid. Cyclooxygenases (COX) are one of the most studied enzymes of medical interest as they are the target of analgesics and anti-inflammatory drugs. Its importance is attested by the fact that John R Vane was given the Nobel Prize (in 1982, along with Sune K Bergstrom and Bengt I. Samuelsson) in physiology and medicine for theorizing that NSAIDS lowered COX catalysis of polyunsaturated fatty acids (1). COX are membrane-embedded heme-enzymes, considered to be highly relevant in both normal cell physiology (signal transduction) and in maladies like arthritis and cancer (2, 3). Also known as prostaglandin-endoperoxide synthases (PGTS), these enzymes convert arachidonic acid (AA, a polyunsaturated fatty acid), released due to the hydrolysis of ester bonds of phospholipids by phospholipase A (or PLA). The products of COX catalysis of AA are prostaglandin (4) and other downstream eicosanoid compounds(5), the precursor of the signaling cycloendoperoxide molecules which are responsible for pain and inflammation (e.g. other prostaglandins like PGD₂, PGE₂, PGF_{2α}, PGC₂, etc.; prostacyclin/PGI₂ and thromboxanes - TXA₂) (Figure 1). AA is also metabolised to form leukotrienes (LTA₄, B₄, C₄ & D₄) through the action of lipoxygenases (LOX), a membranous iron-containing enzyme. Although known to have essential functional roles in normal physiology (6), prostaglandins are also pain hormones and hence, NSAIDs and other molecules which inhibit COX1/COX2 are used as pain killers. While thromboxanes lead to platelet aggregation, prostacyclins prevent thrombosis and blood coagulation and hence, have cardioprotective actions (7).

The two main varieties of COX enzymes – COX1 (PTGS1) and COX2 (PTGS2) are structurally similar enzymes of 70-72 KDa (8) and vary in the nature of expression in different tissues and exert tissue-specific effects through receptor binding and signal transduction (9). While COX1 is constitutively expressed in most tissues and is believed to serve homeostatic functions, COX2 is inducible and expressed during inflammation. Inhibition of the COX isozymes have long served as a popular strategy for the treatment of pain/inflammation, as exemplified by non-steroidal anti-inflammatory drugs (NSAIDs) and other natural as well as synthetic pain killers (10). The active COX dimer is monotonically inserted into cellular membranes like endoplasmic reticulum

(primary site). Human COX-1 and COX-2 are homodimeric proteins with 576 and 581 amino acid residues, respectively (11). The catalytic domain comprises of two distinct active sites – the perox site and the cyclox site (8). Interestingly, while the three-dimensional structures of the two enzyme isoforms are nearly identical, their substrate preferences (reasoned to be owing to variations in cyclox site entry channel residues and presence of a hydrophilic side pocket in COX2), physiological functions and pharmacological actions are understood to be dissimilar (12).

The enzyme supposedly has a Janus (a Roman mythological god of gateways, with two faces) like facet, with two ‘active sites’, a larger (and cave-like) distal heme pocket that opens into the aqueous milieu and (13) a proximal pocket containing Tyr385 that opens towards the membrane via a very narrow channel (schematic is shown in Figure 2, and other COX-structural images in the later part of the manuscript). In the classically acclaimed mechanism, the distal heme site (called herein as perox site, pocket towards the aqueous milieu) acts as a classical peroxidase that directly uses hydrogen/organic hydroperoxides via a 2e mechanism. Going via Compound I formation, this process also generates a tyrosine radical at the narrow channel connected to Y385 from the lipid phase (called herein as cyclox site), which acts as an electron or hydrogen atom abstractor that ultimately inserts two molecules of dioxygen at two distinct loci of AA, the 20 carbon long fatty acyl substrate (Figures 1 and 2). Addition of one O₂ molecule by cyclox site at C13 leads to formation of an endoperoxide product, PGG₂ (product of cyclox site and substrate of perox site), which also contains a hydroperoxide (through the addition of yet another O₂ molecule). This molecule is converted to PGH₂, the final product of COX1/COX2 action, at the perox site (14). Downstream and tissue-specific products of PGH₂ such as PGD₂, PGE₂, PGF_{2α}, PGI₂ (Prostacyclin) and TXA₂ are generated subsequently. For both these peroxidase and cyclooxygenase activities, the heme cofactor is essential.

Via our earlier explorations, we have mooted murburn concept as a fundamental principle of life (attesting that DRS plays obligatory roles in diverse routine physiology) (15, 16) and that several soluble and membrane-embedded redox-active proteins could also work in a similar way (17-24). In connection with this pursuit, in a paper published a few years ago (25), we revisited the known structural aspects of COX enzymes and analyzed the currently accepted mechanistic aspects of its enzymatic role (depicted in Figure 2). AA is liberated through PLA₂ action in the membrane and enters the cyclox site. Discussing the various aspects involved (25): (a) roles of tyrosine radical

versus DRS (diffusible reactive species), (b) observations of mutant proteins on the roles of tyrosine, (c) available evidence for DRS dynamics in cyclooxygenase activity, etc., we had found multiple reasons for projecting that COX enzyme may in fact be a murzyme (defined as proteins that generate/recruit DRS for routine activity). That is: COX enzymes work via not just active site binding-based mechanisms, but also with the intermediacy of oxygen centered radicals and singlet oxygen (collectively called as DRS). When a simple query was presented to the online portal of ChatGPT, worded as: “*What are the unsolved aspects of cyclooxygenase catalytic mechanism?*”, it gave the following summary statement: “*While much is known about the basic catalytic mechanism of COX enzymes, several aspects remain unsolved. These include the detailed peroxide activation mechanism, substrate specificity, allosteric regulation, isoform-specific functions, interactions with other proteins and lipids, precise mechanisms of NSAID inhibition, roles in various diseases, and the identification of alternative pathways and metabolites. Further research in these areas is crucial for a more comprehensive understanding of COX enzymes and their implications in health and disease.*” Notwithstanding our orientations and backgrounds, this foreground presented by modern day “artificial intelligence” justifies our pursuit. We avail evidence for DRS generation/usage from literature in COX system (both COX-1 and COX-2) and use molecular docking studies herein for analyzing the binding of substrates, metabolites and modulators (inhibitors and activators) to the isoenzymes COX-1 and COX-2. To explain COX catalytic mechanism, we propose that it is a murzyme that employs DRS, and thereby, its physiological role is holistically better explained by murburn concept.

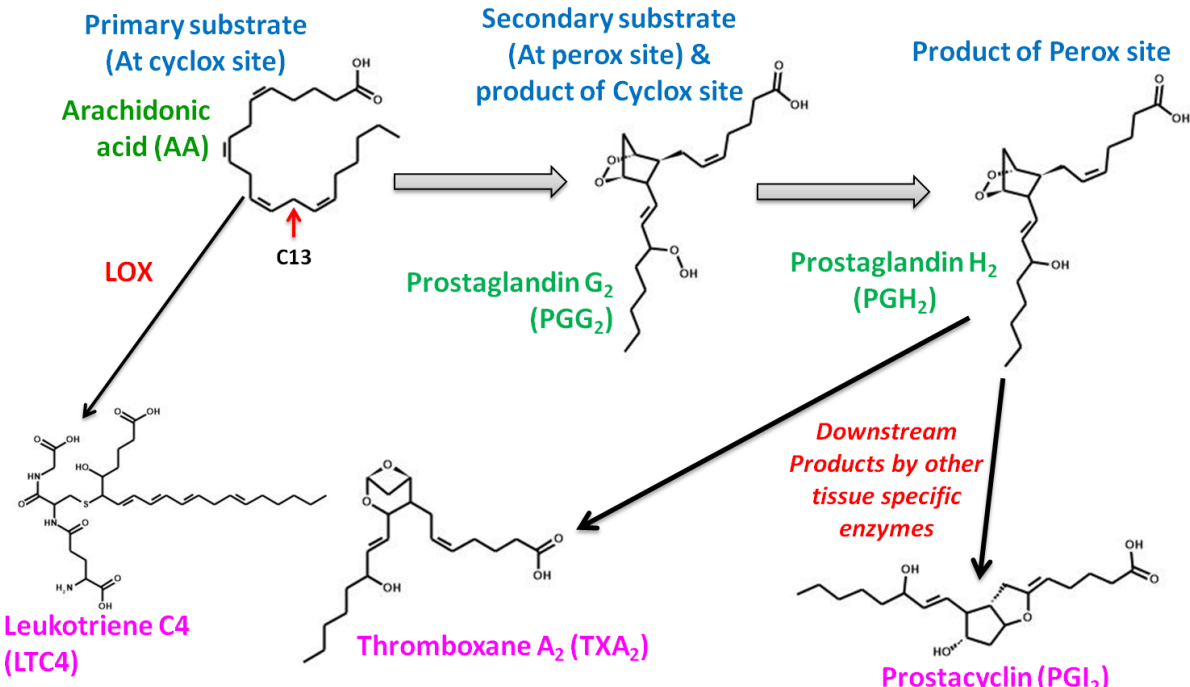


Figure 1: The relevance of COX in the physiology of pain/inflammation signaling. The cascade of enzyme activity is inhibited by NSAIDs, which stop the conversion of AA by COX. LTC4, a product of the LOX (lipoxygenase) pathway, is not a product of COX enzyme action. PGG₂, PGH₂, PGI₂ and TXA₂ are structurally similar entities and hence, there may not be marked distinction in their binding affinities for cycloxo/perox site. The compounds shown here are the substrates which were explored as substrates in the molecular docking studies. LTC₄ was chosen as a negative control, as it is a product of LOX action which is not expected to bind to COX proteins. TXA₂ is a “downstream product”, as it is generated from PGH₂.

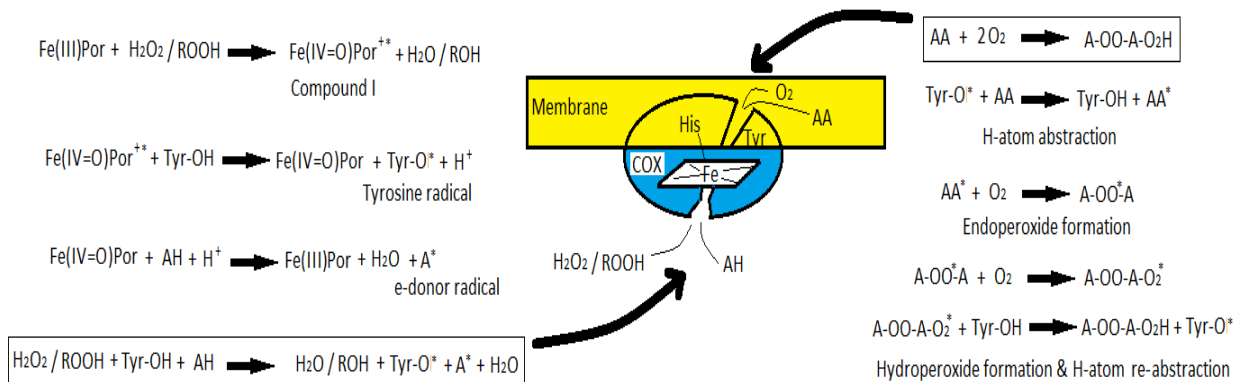


Figure 2. The acclaimed catalytic mechanism of COX enzymes. The enzyme is supposed to use four substrates, two each at each of the active sites. The second step of PGG₂ reaction at perox site (i.e. step 2 of Figure 1, forming PGH₂) is not included here.

2. Materials and Methods

In order to check the binding affinity of cyclooxygenase site inhibitors with cyclooxygenase, crystal structures of 7 COX enzymes from mammalian sources (both COX1 and COX2) were taken from RCSB protein data bank (1CX2, 1EBV, 3KK6, 3N8Z, 5F1A, 5KIR). LogP (a partition coefficient; logarithm of the ratio of concentration of the compound in octanol and water phases) of a hydrophobic compound is positive whereas a negative value of LogP indicates that the molecule is hydrophilic. ADMET-SAR 2.0 (26) and MedChemDesigner 5.5 software ([www. simulations-plus. com](http://www.simulations-plus.com)) were used for prediction of LogP. The molecular structures of 11 well-known COX inhibitors (which are known to bind to the cyclooxygenase site) chosen for this study are depicted in Figure S1. The structures of these molecules were downloaded from PubChem for using AUTODOCK (27), in molecular docking studies. Docking was carried out by considering the AA binding amino acid residues of the cyclooxygenase site. Receptor structures were obtained from the PDB complexes by selecting a single protein subunit and removing all water and co-factor molecules. All heteroatoms (including heme) were removed from the chosen COX1 and COX2 proteins to minimise any interactions between heme iron with the ligands, as this could affect blind docking results. AutoDockTools was used to add hydrogens, calculate Gasteiger charges, and generate PDBQT files. Grids were prepared to accommodate the amino acid residues reported in literature for the cyclooxygenase site (mainly, AA interacting residues) and the entire perox cavity was taken for grid docking. The default grid spacing value of 0.375Å was used, which is about a quarter of the length of a carbon-carbon single bond. Dockings on the whole dataset were run with default LGA settings (10 poses generated). The output was analyzed using ChimeraX and PyMol. TPSA and other molecular properties of substrates and inhibitors chosen for docking studies were determined. The binding affinity of the compounds (substrates and inhibitors) was compared using both blind docking and grid docking approaches. All other procedures/details for molecular docking are as given in a previous publication (20).

3. Results and Discussion

Before interpreting the results obtained in this study, the reader is advised to peruse the elaborate explorations our group carried out (theoretical, *in silico* and experimental) with diverse

heme-peroxidases (28) and membrane-embedded cytochrome P450s or CYPs (29, 30), which established the murburn mechanism for physiological heme-enzyme functioning. Therein, we had shown that diverse molecules could get converted by the heme enzyme without the former gaining access to the active site [wherein the native oxidation state is Fe(III)]; also, reasoning that rather than going via a two-electron mechanistic cycle involving an enzyme-centric Compound I [logically akin to an Fe(V) species], the enzyme could also recycle via a one-electron [Fe(III)-Fe(IV) species] scheme with the involvement of DRS. These findings are very relevant for understanding and explaining the current results and mechanism of COX enzymes. The most salient aspect of our earlier explorations of peroxidase structure-function is that DRS are not merely futile and accidental by-products of oxygen metabolism by heme enzymes, but are central to the cellular metabolic chemistry (16, 22, 28, 30).

3.1. Revisiting the structure-functional aspects of classical COX mechanism

Herein, we mostly present images with the human COX isozyme structures in the main manuscript and depict images of the mammalian counterparts in the Supplementary Information. However, some figures dealing with murine COX are also introduced into the main manuscript, as crystal structure with AA embedded within the cyclox site is only available in this system.

COX1 and COX2 are often 3-4 N-linked glycosylated dimeric proteins. Each monomer of the functional dimeric enzyme contains three prominent domains: epidermal growth factor domain (residues 34-72), membrane binding domain (residues 73-116) and the catalytic domain, which is comprised of the rest of the ~570 odd amino acid structure. Both COX isoforms are almost superimposable, possessing very minor structural differences and sharing a sequence identity of 60%. While AA is an achiral substrate, the product of cyclox site - PGG₂, is a bicyclic endoperoxide which contains five chiral centres (31). The substrate - AA and other fatty acid substrates are deemed to be positioned very close to the conserved Y385 residue. AA binding and subsequent positioning in the productive pose then leads to abstraction of a 13-proS H-atom by Y385* (tyrosine radical). The oxidant at the peroxy site can be any of the three - hydrogen peroxide, an alkyl hydroperoxide, or peroxynitrite (32). An alkyl hydroperoxide (ROOH) substrate, when bound to the peroxy site, oxidises heme iron to cause formation of a Compound I radical (subsequently leading to the release of ROH/PGH₂); further one-electron oxidations of peroxidatic

substrates lead to regeneration of heme. Y385* is supposedly generated when it transfers an electron to Compound I, similar to that of heme peroxidases (33). The Y385* causes the generation of an allyl radical of AA, which attracts molecular oxygen to form the cyclic endoperoxide(34). The transfer of an electron to generate the Y385* in COX1 (and correspondingly, Y371 in COX2) is considered to occur through electron tunneling. The cyclox entry channel is just 6-8 Å wide and the L-shaped cyclox cavity is ~25 Å deep, while the heme cavity (perox site) is much broader (35). The crystal structure of substrate (AA)-bound mCOX2 is shown with the N-glycosylation sites in Figure S2 (PDB ID: 3HS5). One peroxidase turnover event supposedly generates the catalytic tyrosine radical and this makes the cyclooxygenase reaction (with synchronous action of both perox and cyclox sites) self-perpetuating (11, 12). Apparently, only one of the monomers (of both isoforms) contains heme, while the other monomer (that is devoid of heme) supposedly serves an allosteric role. An intriguing perception in the field is that the efficiency of AA bound to one of the monomers is dependent on the nature of the competing fatty acid bound within the allosteric monomer (36). One wonders why this mechanistic necessity should arise or be conserved across the systems. The finer details of the erstwhile mechanism of COX enzyme action can be accessed elsewhere (12, 34).

3.2. Partitioning profiles of substrates, products, control molecules and their docking/binding at the cyclox/perox sites of COX

Both substrates and inhibitors are known to gain access to the secluded (and membrane-oriented) cyclox site from within the membrane (37). As the logP value for AA is >6 (Table S1, Supplementary Information), the vast majority of the limited amount of arachidonate (released by PLA action) would reside in the lipid phase. As the openings to the cyclox site lies in the extra-membrane aqueous region of COX (Figure 3), the propensity for the bulk lipid-phase AA to diffuse into the constrained cyclox site would be minuscule. (Contextually, the observation of X-ray crystal structures of murine COX with AA located inside the protein's cyclox site has very little relevance, as such structures are obtained with unrealistic protein-ligand mixtures that are kept over long time, and after subjecting the mixture to gradual removal of water!) Also, PGG₂ & PGH₂ (logP > 4), would prefer to reside majorly in the lipid phase rather than the protein's hydrophilic perox active site that is exposed to aqueous milieu. According to the conventional hypothesis, the organic

hydroperoxide PGG₂ must bind directly to heme iron in the rather hydrophilic and water-accessible perox cavity (38, 39). For the realization of the proposal above (since there exists no direct route for PGG₂ to wade through the back of the cyclox site into the perox cavity), the interim product must deterministically exit the cyclox site the same way it entered, and then perhaps exit the membrane – and finally, make its way around the protein surface to access the perox site, via the aqueous phase (38).

The primary substrate AA (of cyclox site; the starting material for COX catalysis), intermediary substrate/product PGG₂ (product of cyclox site and substrate of perox site), final product PGH₂ (the product of perox site and overall COX catalysis), and downstream tissue-specific products (PGI₂ / TXA₂ / PTC) were docked to both cyclox and perox sites. Ideally, AA binding at cyclox site and PGG₂ binding to the perox site must be favoured, as these are the respective substrates for the corresponding sites of the COX protein's classical catalytic cycle. The rationale is that substrate binding should theoretically have lower ΔG values than product molecules. Also, the control products of COX catalysis - leukotrienes, thromboxanes and prostacyclins (which are not substrates of cyclox site but are downstream products of the inflammation pathway), would not be expected to show significant binding at the active site (40). From literature, it can be seen that AA purportedly adopts an L-shaped binding pose within the constrained cyclox site (41). Quite contrary to such expectations of classical perceptions (40), we found that (Table 1 & Table S2):

- (i) AA did not dock to cyclox site,
- (ii) except for sheep COX1, PGH₂ docked to both cyclox and perox sites in all COX proteins,
- (iii) except for human COX2, effective differentiation of PGG₂ over PGH₂ could not be established at the perox site,
- (iv) except for a human COX2, all COX proteins showed effective binding of PGH₂ to the cyclox site,
- (v) there existed considerable variations in the binding/differentiation ability of substrates/products of COX1 or COX2 across the species,
- (vi) discernible differentiation could not be obtained for substrate/product docking profiles of the human COX1 versus COX2, and

(vii) the downstream products of PGH₂ metabolism (controls) showed significant and non-discriminable binding preferences/variations.

These results question the classical active site mediated catalytic logic, but may be explained by murnburn mechanism.

Table 1: Grid-centered docking data of substrate and product molecules with various COX enzymes (higher relative affinity of a given ligand for a given COX is highlighted in bold)

Protein & Source	Ligand	Perox site		Cyclox site	
		ΔG (kcal/mol)	K _d (μM)	ΔG (kcal/mol)	K _d (μM)
COX1	3KK6 (sheep)	AA	-	-	-
		PGG ₂	-6.5	17.2	-9.2
		PGH ₂	-7.3	4.0	-6.5
	1EBV (sheep)	PGG ₂	-	-	-9.3
		PGH ₂	-	-	-9.4
	3N8Z (sheep)	PGG ₂	-7.0	5.2	-7.3
		PGH ₂	-7.3	4.2	-6.6
	6Y3C (human)	PGG ₂	-8.5	0.5	-6.1
		PGH ₂	-8.3	0.8	-8.4
COX2	5KIR (human)	PGG ₂	-7.6	2.3	-6.8
		PGH ₂	-6.5	15.3	-3.4
	5F1A (human)	PGG ₂	-9.4	0.1	-7.8
		PGH ₂	-8.2	1.0	-8.0
	1CX2 (mouse)	PGG ₂	-7.3	3.9	-7.1
		PGH ₂	-8.7	0.4	-6.8
					10.4

Almost all fatty acid substrates, including AA, are presumed to adopt the L-shaped contorted structure within this binding pocket involving almost the same residues in both COX1 and COX2 (12). Within the same dimeric crystal structure of mCOX2 – 3HS5 (Figure 3), AA adopts two different poses within two different monomers, one favourable and another unfavourable (42). Favourable AA binding to the cyclox site involves multiple non-covalent interactions, with the proximal (involving C-atoms 1-7 of AA), central (C-atoms 7-15 of AA) and distal (C-atoms 15-20 of AA) atoms interacting with a set of amino acid residues of COX enzymes. As COX1 is known to possess a smaller cyclox site, it supposedly favours majorly AA binding, while COX2 is able to bind to and catalyze other diverse fatty acids like linolenic acid, linoleic acid, EPA (eicosapentanoic acid) and DHA (docosahexanoic acid) owing to its roughly ~20% larger active site (43, 44). However, since most of the active site residues are almost identical in both isoforms, it is plausible that there would be no large differences in substrate binding preferences of COX1 and COX2 (Figure 3 and Figures S4-S6). Interestingly, DHA adopts the same L-shaped

conformation and almost the same binding pose as AA, and is still a poor substrate (35). Among the 24 odd residues distributed within the active sites of both COX1 and COX2, I523 is present in COX1 and the slightly bulkier V523 side chain is seen in COX2 cyclooxygenase active site. This factor is attributed to be responsible for the substrate binding discrimination of the two enzymes (45). [[Other than this, the active site amino acids of both the enzymes are identical; the residues involved in AA binding that are present within the cyclooxygenase cavity are L117, R120, F205, F209, V344, I345, Y348, V349, L352, S353, Y355, L359, F381, L384, Y385, W387, F518, I/V523, G526, A527, S530, L531, G533 and L534 (46).]] While comparing the aligned key active site residues of COX-1 and COX-2 from different mammalian sources (Figures S4-S6) and in comparison with earlier literature (47), it is clear that there are only minor active site volume as well as electrostatics variations within the cyclooxygenase pocket. There is a deep labyrinth within cyclooxygenases, which has not just the membrane-embedded cyclooxygenase channel, but also contains other alternative channels, whose functioning is not known (Figure 4). COX1's narrower entry channel (with residues such as 1434, H513 and I523, COX2 has V434, R513 and I523) is compared with the slightly wider COX2 channel and adjoining sub-pocket (Figure 5). These differential aspects of hCOX1 and hCOX2 active site channels/peripheries and substrate positioning are compared in Figures 3, 4 & 5 and Figure S3.

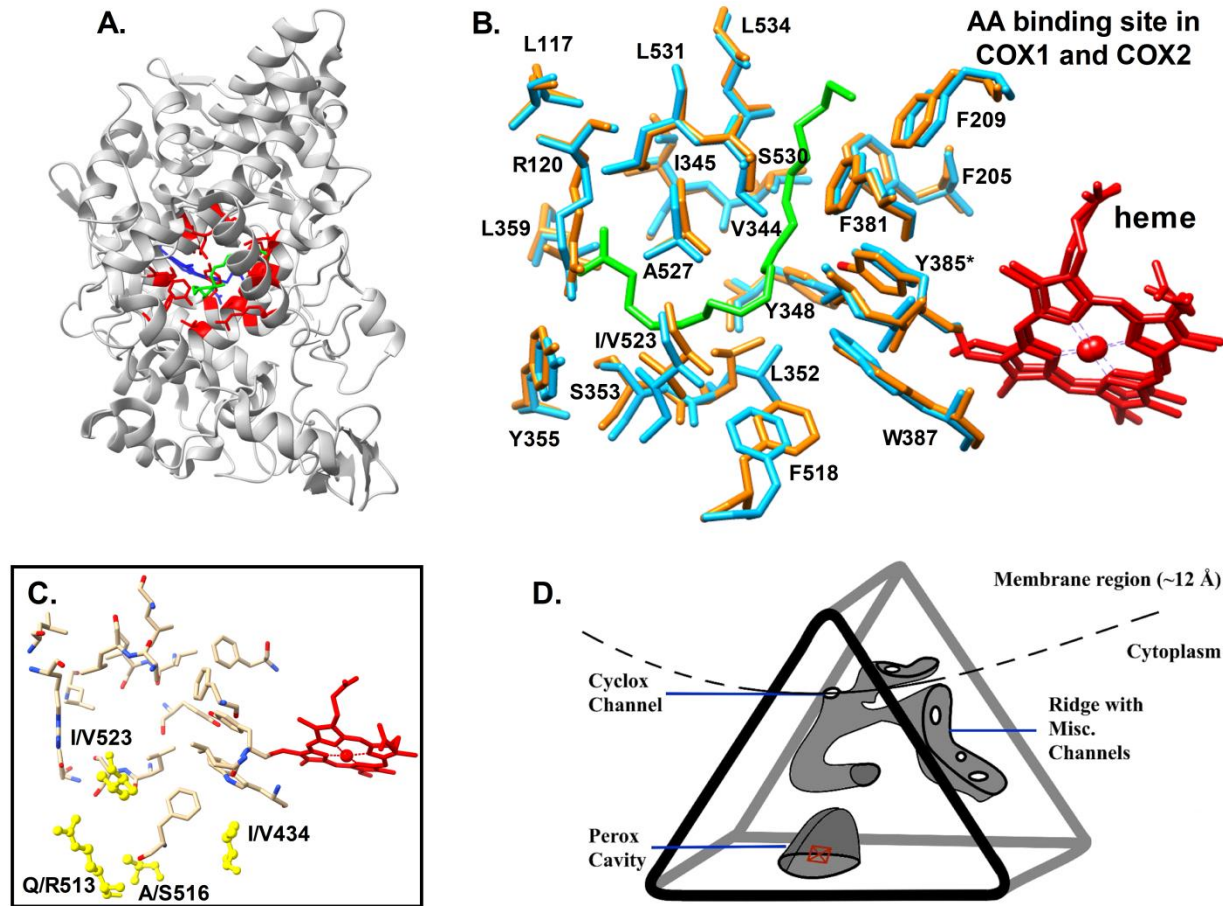


Figure 3. Analysis of general structure and cycloo-perox sites of cyclooxygenases. A. Ribbon structure of mouse COX2 (PDB ID: 3HS5) showing the residues involved in AA binding (red), bound AA (green) and the heme (blue). B. Superimposed residues involved in AA binding; orange sticks – human COX1 (PDB ID: 6Y3C) and blue sticks – human COX2 (PDB ID: 5F1A). The green stick is AA bound to the superimposed structure of mCOX2, whose residues are hidden and only AA is shown to give a perspective of AA binding to the cycloo pocket of the two enzymes. C. The hCOX residues involved in AA binding are coloured by atom (N-blue, O-red and the entire heme ring is coloured in red). The residues marked yellow are different in COX1 and COX2 (only atoms of COX2 are shown). Except for one residue which is different between hCOX1 and hCOX2 among the active site residues (I/V523), there is not much of a difference in the AA binding pocket. D. Analyses of cavities in hCOX1 and hCOX2 – The cavities and openings on the protein surface were compared for the two proteins. The narrow cycloo channel leads to a wide hydrophobic pocket which leads to a few miscellaneous channels which also open into the common pocket. These miscellaneous channels may not allow movement of PGG₂ out of the protein, and hence, the product of the cycloo site can only leave through the same entry channel. The perox cavity is a much larger, cave-like pocket containing heme. There does not seem to be any connection between the perox and cycloo site, but DRS can percolate through the protein. These features are quite akin to the DRS-channels in the heme-thiolate drug-metabolizing enzymes, cytochrome P450s (48).

Several fatty acids with varying chain lengths, number of *cis*-double bonds starting at differing carbon atom number (starting from the non-carboxy end!) like: arachidonic acid [AA 20:4 (n-6)], eicosapentanoic acid [EPA 20:5 (n-3)], dihomo-gamma-linolenic acid [DGLA 20:3 (n-6)], alpha-

linolenic acid [ALA 18:3 (n-3)], linoleic acid [LA 18:2 (n-6)], mead acid [MA 20:3 (n-9], docosahexanoic acid [DHA 22:6 (n-3)] are metabolised by COX enzymes. It is impossible to envisage how these diverse molecules could all bind to the cyclo-x-site and get specifically and selectively inserted with diatomic oxygen. But if we imagine them transiently docking or approaching them near the various apertures of the DRS-channels we point out herein (Figure 4), then the catalytic mechanism becomes highly accommodative of the observations seen in physiology.

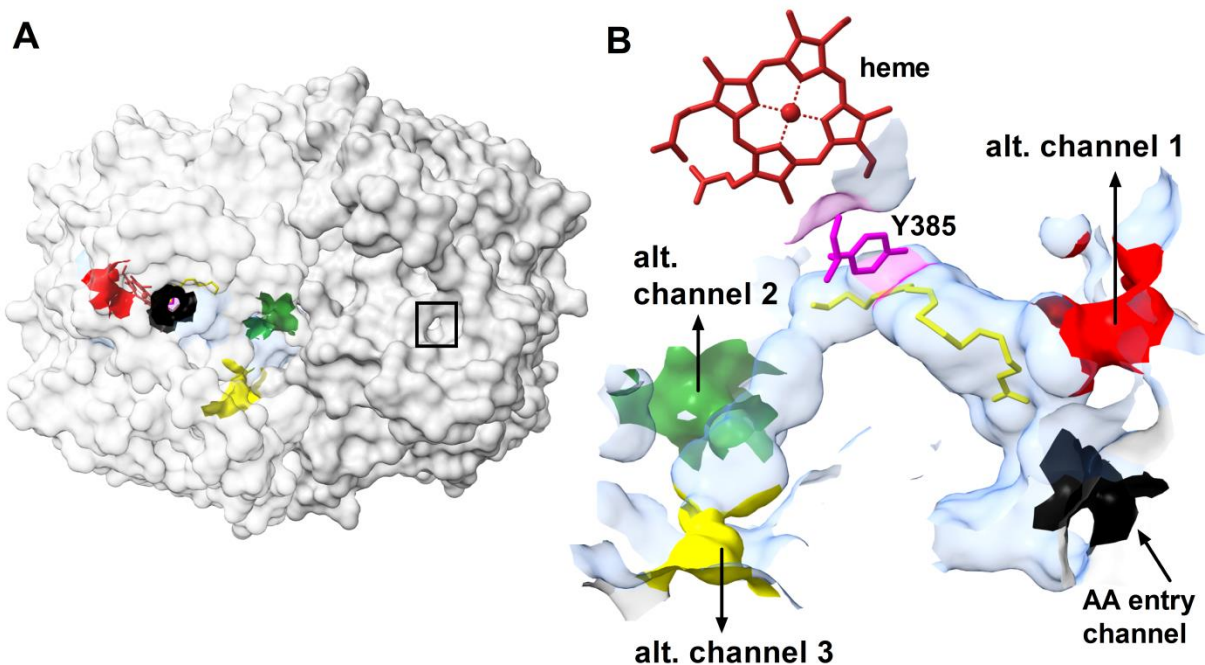


Figure 4. AA entry channel, internal cavity labyrinth and alternative channels. While the labyrinth in mCOX2 (PDB ID: 3HS5) was made transparent, the mouths of the channels were not made transparent. The AA bound inside is shown as a yellow stick and the critical Y385 residue is coloured magenta. In all these channels and within the labyrinth, several narrow constrictions can be seen, which can limit the movement of the substrates, products and inhibitors. The AA entry channel is very narrow and is constricted, but the alt. channel 1 is not; this channel leads to the membrane side, but is not likely to be associated with the membrane like the AA entry channel is. The other two alt. channels 2 and 3 open into the dimeric interface. AA and its product, PGG₂ could be hindered by the amino acid side chains within this twisted cavity. Such a feature would be useful only for DRS-dynamics in murzymes.

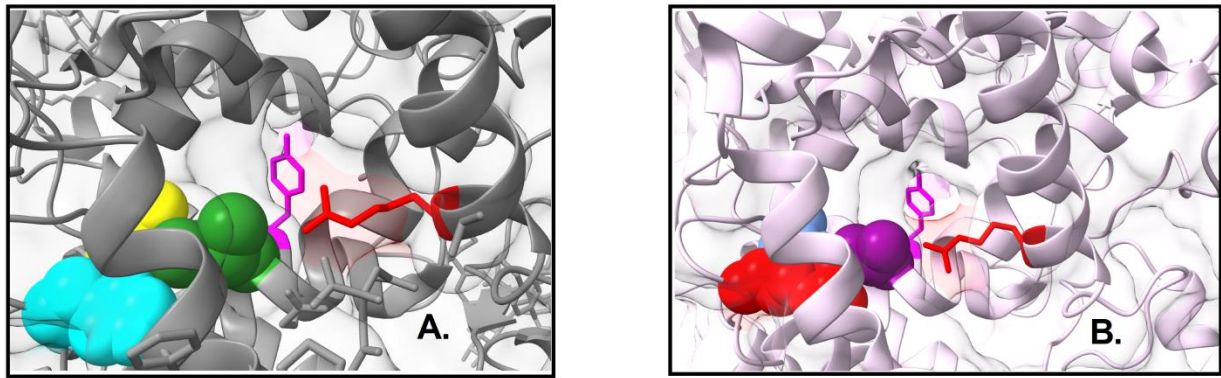


Figure 5. Analysis of access channel and side pocket residues of cycloxygenase sites of hCOX1 and hCOX2. The cycloxygenase active site access channels and side pockets of hCOX1 (left) and hCOX2 (49) are depicted. A. In hCOX1, the atoms of the side chains of I523 (green spheres), H513 (cyan spheres) and I434 (yellow spheres) are shown. B. At the same positions, the variable amino acid residues of hCOX2 are shown – V523 (purple spheres), R513 (red spheres) and V434 (blue spheres). In both A and B, Y385 is coloured as a magenta stick and R120 is coloured as a red stick. The variable V/I523 is not shown.

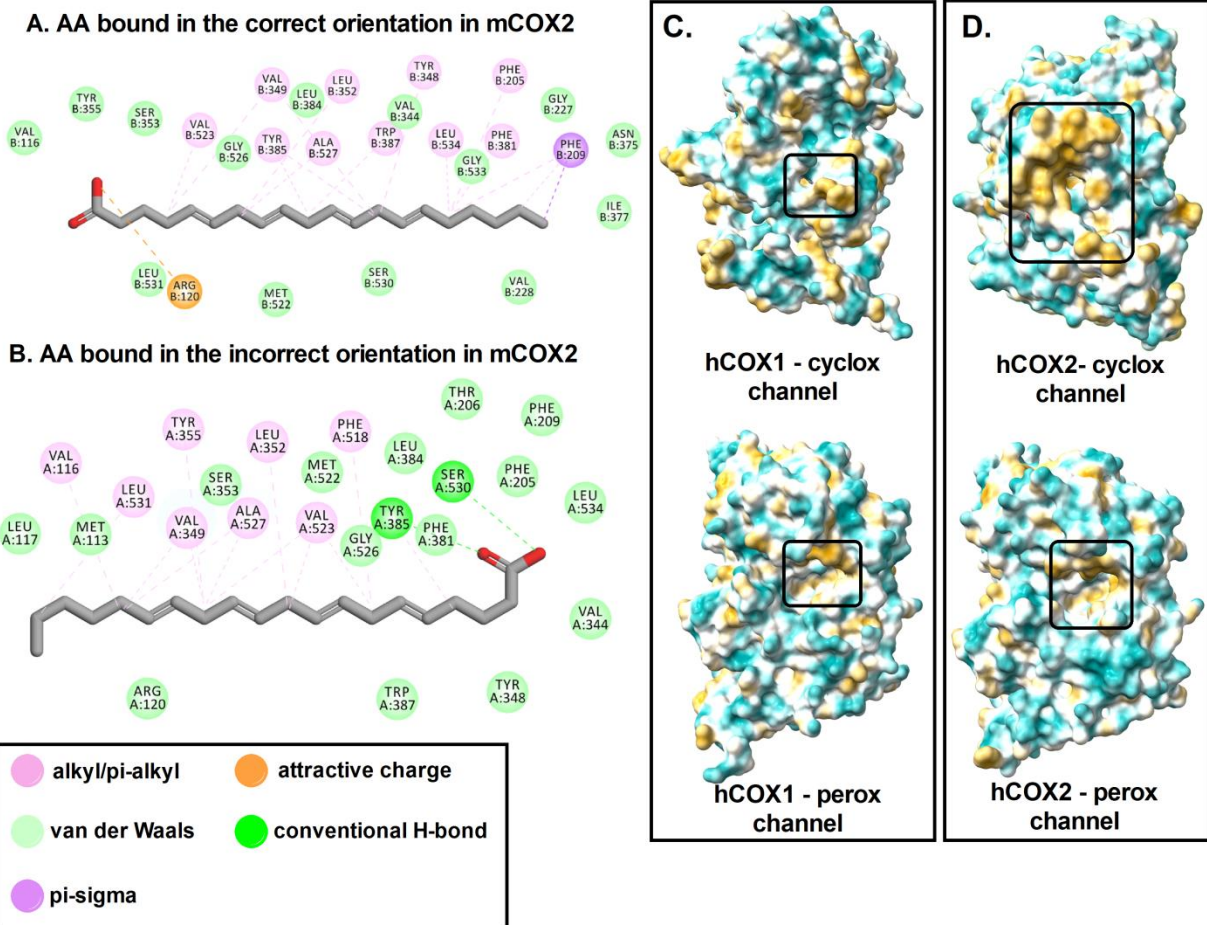


Figure 6. AA binding in mCOX2 (3HS5) – In the crystal structure of mCOX2, AA had bound to both monomers in the correct (panel A) and incorrect orientation (panel B) within two different monomers of mCOX2 (3HS5). The images within the boxes show comparison of COX1 and COX2 cyclooxygenase surfaces at the Cyclox and Perox cavities. When comparing the hCOX1 and hCOX2 surfaces (C and D), the hydrophobicity of hCOX2 cyclox channel is higher than that of the hCOX1 cyclox channel.

Apart from AA (shown at 3 O'clock position in Figure 7), the unsaturated fatty acids such as EPA (eicosapentaenoic acid) (35), AA (arachidonic acid, the most popular substrate), GLA (γ -linolenic acid) (50), DTA (docosatetraenoic acid) (51, 52), DH-GLA (dihomo- γ -linolenic acid) (51), LA (linoleic acid) (53), ALA (α -linoleic acid) (53) and DHA (docosahexaenoic acid) (35) are known to act as substrates of COX enzymes.

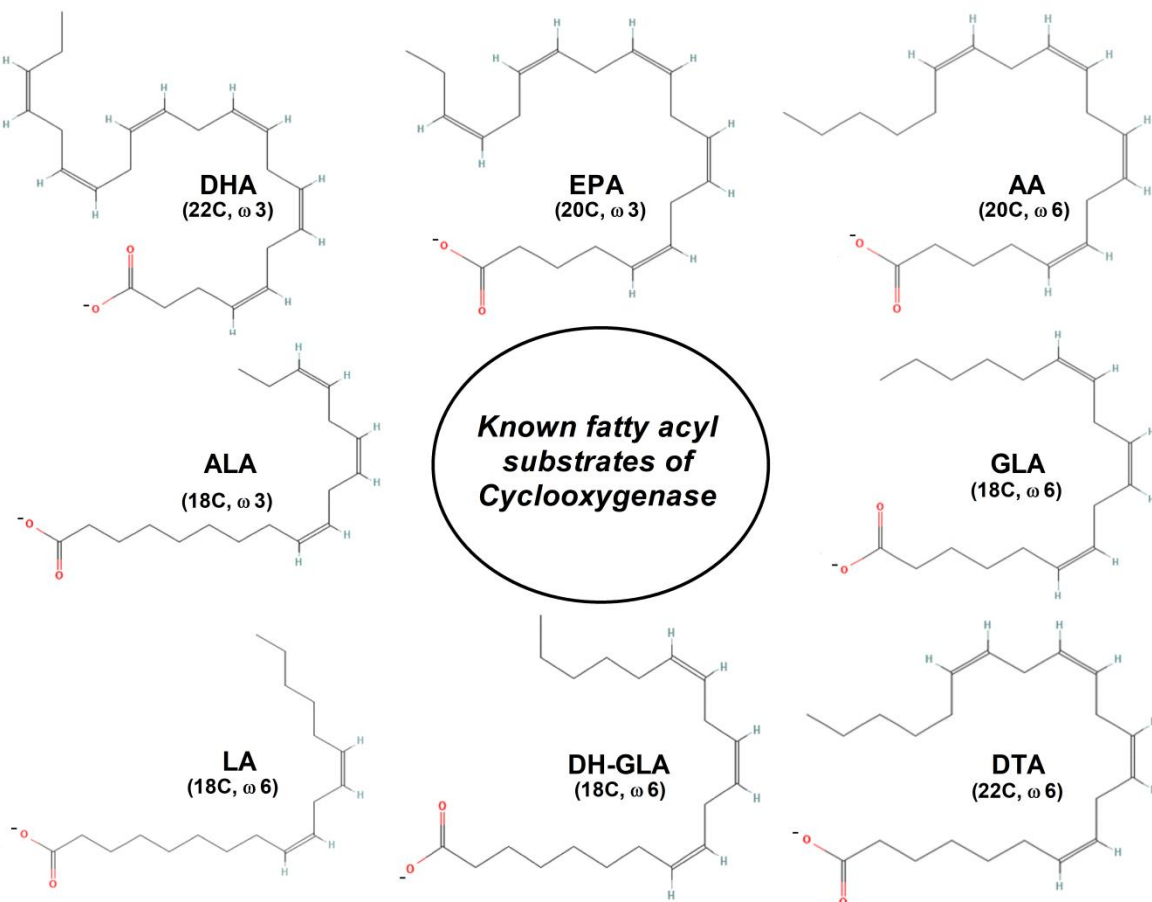


Figure 7. Structure of some known fatty acyl substrates of COX enzymes

It can be seen that the double bond from the acidic carbon moiety (the stabilizer of binding of the substrate, by virtue of forming a salt-bridge with arginine at the entrance of the cyclox-site channel) is located at various lengths (3 to 8 sp^3 bonds!) from the olefinic carbon (the site of

attack). Not only that, the double bonds and the fatty acyl chain length vary considerably among the substrates, all of which cannot enable a favorable positioning of the substrate close to the purported Tyr385 residue. In the table shown in SI materials (Table S3), the details of fatty acids that were reported to act as substrates and inhibitors are presented. Some of these fatty acids are deemed to be “allosteric modulators” of COX function (54). These fatty acids are structurally diverse in aspects such as - carbon chain length, number of double bonds, omega type (3/6/7/9), etc (Table S3). It is asking for an inexplicable super-intelligent enzyme to bind to such diverse fatty acids and subject itself through the most extraordinary induced-fit type of mechanism to enable the improbable positioning of substrates close to bonding distance with the purported Tyr385 residue. It is also asking for yet another marvelous mechanism to imagine that once the first oxygen molecule gets inserted, the substrate somehow moves or the enzyme reorients itself to insert oxygen on another site of the substrate. On the other hand, it can be easily envisaged that non-specific binding/presence of the fatty acids close to the DRS-apertures of the COX proteins (Figure 6) could enable them to get converted via murburn chemistry, and this could also explain the inhibitory effects of other fatty acids.

3.3. Meta-analysis of literature data on COX and its mutants

We surveyed the voluminous data on COX and its mutants, and attempted to make holistic sense of its function.

a) Mutation/alteration of residues involved in catalysis and substrate/inhibitor binding

A salient aspect that begs attention is the mechanism of tyrosine radical generation from AA. There are over 27 tyrosine residues in both COX1 and COX2, and two tyrosine residues are located very close to the heme centre – a) Y385, which is 12.6 Å away and b) Y409, which is merely 10 Å from heme, and is located in the heme cavity. Another aspect is the arginine (R120) residue at the mouth of a channel. Mutagenesis or modification of several other tyrosine residues in COX enzymes yielded quite interesting results. Treatment of cyclooxygenase with tetranitromethane led to nitration of tyrosines and abrogation of cyclooxygenase activity. However, treatment with competitive inhibitors of cyclox activity, such as ibuprofen and indomethacin, prevented

tetrinitromethane-induced inactivation (55). These findings suggest that ibuprofen and indomethacin competed with the DRS, and their presence in the reaction mixture (along with COX) offered the escape from the tetrinitromethane reaction.

When the critical Y385 residue was mutated to phenylalanine, there was 0% cyclox activity and intriguingly, even the peroxy activity diminished by almost 43%. Moreover, three tyrosine residues, Y355, Y385 and Y417 were also mutated to phenylalanine in that work (55) [in agreement with the popular six-step “all radical” mechanism given by Hamberg and Samuelsson (12)]; and the mutants showed various levels of loss of cyclox activity and gain/loss of peroxy activity. However, another group reported that Y385F mutant of COX1 did not abolish the peroxidase activity of the enzyme and affected only the cyclooxygenase activity (56). Such observations do not consistently support the erstwhile mechanism. Very dramatic alterations in the lifetime of tyrosine radical were observed with addition of cyclox site inhibitors such as nimesulide (>10 hrs.), flurbiprofen (48 min.), etc. (compared to ~4 minutes in the control). In the same study, substoichiometric levels of nimesulide were found to elevate the lifetime of tyrosine radicals; additionally, another tyrosine radical, Y504, was detected in the presence of nimesulide (57). These seem to suggest a delocalised and DRS-mediated mechanism for tyrosine radical generation, *per se*! In our viewpoint, the lifetime of the DRS generated at the heme site (or the DRS entering the cyclox site) could be prolonged by tyrosine radical formation.

The amino acid side chains of R120, S353 and S530 are supposed to facilitate AA binding whereas R120, E524 and Y355 are considered important for normal cyclox activity (58). The arginine group of R120 presents a positive charge which forms a salt bridge with E524, and also stabilises the carboxylate head of fatty acid substrates. Mutation of R120 (R120K, R120Q and R120E) affected COX-1 activity, leading to increase in K_M and significant loss of activity. When 20 odd residues interact (Figure 6), it is inconceivable how the R120 located at the entry of the channel would so significantly affect cyclox activity. The explanation that modification of R120 disrupts the stabilization of COO^- group of fatty acid substrates (59) is questionable. When R120 was mutated to lysine (R120K), K_M still increased 20 folds and cyclox activity decreased by 85% (12, 58). Ideally, if charge stabilization involving R120 was so crucial, R120K mutation should not have significantly affected cyclox activity. Besides, R120 is at the entry channel and far away from

the tyrosyl radical which is placed almost 20-25 Å deep inside the cyclox cavity. With the omega end of the fatty acid going into the active site, the hydrophobic interactions would not be majorly affected. This is just one of the many examples of mutations in several sites of the enzyme - entry channel, lobby, proximal, central as well as distal pockets which have been studied in the COX systems. The lobby region (lying close to residues 70-110) is demarcated from the active site by three prominent residues – R120, Y355 and E524 (60). Free COX enzymes (which do not have any ligand) seem to have a closed active site entry channel (as indicated by crystal structure of uninhibited mouse COX2, PDB ID: 5COX). The image shown in Figures S7 reveals the ‘closed’ cyclox active site channel; however, the mouth is presumed to open up to accommodate substrates and inhibitors. V89 of the lobby region, which is located at the mouth of the cyclox channel, was found to be crucial for the entry as well as exit of some inhibitors (61). One more interesting fact is that the crystal structures of substrate bound as well as free COX enzymes (both COX1 and COX2) show no major changes in protein conformation (62). Hence, there does not appear to be any dynamic flexibility for the enzyme to accommodate substrate/inhibitor molecules. Moreover, several mM concentrations of drug molecules as well as fatty acid substrates are added to obtain ligand complexes of COX proteins for NMR, mass spectrometric and X-ray diffraction studies (54, 63). Other non-physiological molecules are also added to induce crystal formation (64) and hence, ligands are “forced” to bind to the protein. These data, therefore, may not reflect the exact mechanism by which redox enzymes such as cyclooxygenases act in the physiological realms, wherein AA would be available at very low concentrations.

The mutation of a glycine residue to serine (G526S) far away from Y385, located at the mouth of the cyclox channel led to formation of products other than prostaglandins, which lacked the cyclic endoperoxide (65). This does not sit well with the conventional hypothesis. Even more perplexing, the results of certain sheep COX1 mutants from a study demonstrate that single and combination mutations of certain amino acid residues which are unrelated to Y385 also cause drastic decline or enhancement of AA oxidation reactions (53). In this interesting work, against the oxidation rates of 100, 15 and 44 observed for AA, EPA and LA (respectively) for the WT ovine COX2 enzyme, F205A mutation led to just 28, 7.5 and 3.5% rates. The double mutant of V349A/S353T yielded just 3, 0 and 0 oxygenation rates for AA, EPA and LA, respectively. F381A mutant exhibited 4, 2.6 and 0.88 (respectively for the three substrates in the order given earlier) and oxidation of all

three substrates was abrogated in the W387L mutant. Even more bizarre is the fact that in the Y355F mutant, AA oxidation rate was 193 (almost double of WT) and W387F mutation increased AA oxidation by four folds! The relative positions of these residues in human COX1 are indicated in the Supplementary Figure S8 (relative to the position of Y385). While on average, there are around 3% tyrosine residues in proteins, there are 27 tyrosine residues in COX proteins (Figure S9) and this is almost 4.5% of all the amino acids. These data question the root assumptions of the classical proposal wherein the substrate interaction occurs only at the tyrosine-centered active site. They could be reasoned with the postulation of involvement of DRS-dynamics, as espoused by murburn model for heme-enzymes.

b) Mutation of Asn residue involved in glycosylation

When a critical N580 residue was mutated in COX2, the cyclooxygenase activity of the enzyme increased by five times that of the WT enzyme (66). This residue is located on the surface, and it may not be even affecting the association of the enzyme with the membrane, as it is far away from the membrane domain region. This N580 mutant COX2 (N581 in the analyzed crystal structure of hCOX1) was also found to be less susceptible to inactivation by COX2-specific inhibitors (67). Figure S10 shows that the N581 residue is nowhere near the cycloxygenase channel and therefore, the mechanism by which mutation of this residue enhanced enzyme activity almost five times is very puzzling. Such observations are inexplicable with the conventional hypothesis, as the site of cyclooxygenase oxygen-insertion activity occurs within an active site that is 25 Å deep. In the murburn purview, oligosaccharide chains present on enzyme surfaces can modulate DRS and thereby, can modulate cyclooxygenase reaction outcomes; the conventional hypothesis does not offer any clear explanation. Mutation of N-linked oligosaccharide attachment residues – N181 and N197 (and T183 as well as T199) on the prion protein PrP^C caused it to scavenge DRS poorly, and sensitised HeLa cells to apoptosis(68). Thus the murburn model also explains pan-systemic observations of similar kind.

3.4. Binding/effect of inhibitors

Pharmacological agents which act on COX systems are classified into the following categories: COX1 specific, COX1 preferential, non-selective (act both on COX1 and COX2), COX2 preferential and COX2-specific. The classification of the 11 inhibitors chosen in the current study (33) and the data obtained herein for docking affinity are shown in Table 3 (and the ratio of impact on COX1 and COX2 activities are given in Supplementary Information). The pharmacokinetics properties of the chosen COX inhibitors are given in Table S4. Many cyclooxygenase inhibitors reportedly bind deep into the cycloxx site, as demonstrated by crystal structures (as well as molecular docking studies); they do not merely dock into the cycloxx channel, as demonstrated by the amino acid residues which dock flurbiprofen and ibuprofen (1). These inhibitors were shown to interact with Y385, S530, W387, E524, R120 and Y355 – some of the very same key active site residues of the cycloxx site involved in fatty acid substrate binding. While some reports argue that carboxylate groups of inhibitors hydrogen bond to R120, a methyl ester derivative of indomethacin was much more potent against an R120A mutant, than against WT-COX2 (69). If the classical classification mechanism were operational, R120 mutation should abrogate AA binding and catalysis in the protein. (One wonders why this experiment was carried out if R120 was that crucial!) Results from such studies only demonstrate that mutations of particular amino acid residues do not concretely establish the exact mechanism of COX enzyme action. Interestingly, even acyl coenzyme A conjugates of ketoprofen inhibit cyclooxygenase by binding to the cycloxx active site (70). Oddly, though many cycloxx site inhibitors interact with and bind to the same pocket, their inhibition constants vary dramatically (71) (and its correlation to the experimental inhibitory effect also, as demonstrated in IC₅₀!); and the only explanation afforded is their ability to bind to and interact with a bunch of amino acid residues.

Table 3: Grid docking to cycloxx site – inhibitors binding to mammalian COX1 and COX2 proteins. Keeping 100 μM as a cut-off value for discriminating as good vs. poor binders, the combinations of receptor-ligand with poor K_i values determined are marked in asterisk whereas the ‘dollar’ superscript highlights discordances in preferential binding to either COX1 or COX2 (that is not expected, based on the class of the concerned inhibitor).

Ligand	COX1 K _i (μM)				COX2 K _i (μM)			
	3N8Z, sheep	1EBV, sheep	3KK6, sheep	6Y3C, human	5F1A, human	5KIR, human	4PH9, mouse	1CX2, mouse
CCB [#]	5.7	1.0	0.1	-	87.0 ^{\$}	1.0 ^{\$}	195.0 [*]	19.1 ^{\$}
RCB [#]	0.2	0.2	0.1	0.8	26.7 ^{\$}	1.0 ^{\$}	72.3 ^{\$}	6.8 ^{\$}
VCB [#]	0.1	0.3	0.2	-	40.4 ^{\$}	1.0 ^{\$}	178.0 [*]	4.7 ^{\$}
NMS [#]	3.8	0.2	1.5	2.0	329.5 [*]	3.9 ^{\$}	4.5 ^{\$}	539.0 [*]
MXM [#]	1.0 ^{\$}	1.6 ^{\$}	14.7 ^{\$}	0.4 ^{\$}	73.3 ^{\$}	5.7 ^{\$}	74.5 ^{\$}	25.0

NBM#	0.5	0.8	16.5	2.3	808.0*	0.3	4.3	102.0*
DCF [#]	95.0 ^{\$}	1.8 ^{\$}	16.0 ^{\$}	1.8 ^{\$}	221.0*	11.3 ^{\$}	73.6 ^{\$}	28.0
SDS [#]	6.7	0.6	3.3	-	70 ^{\$}	4.0 ^{\$}	15.7 ^{\$}	363.6*
PXC ^{\$}	2.2	1.5	42.7 ^{\$}	0.2	624.0*	1.0 ^{\$}	7.0 ^{\$}	25.0 ^{\$}
IMC ^{&}	34.0 ^{\$}	0.1 ^{\$}	4.8 ^{\$}	0.1	134.0*	1.8 ^{\$}	90.3 ^{\$}	539.0*
NPX [@]	3.6	1.0	24.0	1.9	19.5	7.0	18.5	308.6*

Key:

[#] COX2 specific/preferential drugs

^{\$}COX1-preferential drugs

[&]COX1-specific drug

[@]non-selective (inhibits both)

It is notable that all the molecules docked well to the cyclox entry site in COX1, while some COX2-specific inhibitors (shaded in red) docked poorly to COX2 (Figure S11). For example, indomethacin binds via a two-step mechanism of slow and tight binding to both COX1 and COX2, but is not supposed to bind favorably to COX2 (1); while this expected trend is seen for three of the four mammalian COX2 receptors, a K_i of 1.8 μM was obtained with human COX2 (5KIR). Nimesulide, along the expected lines, bound well with one structure of mouse (4PH9) and human (5KIR) COX2, but it bound very poorly to the other two COX2 proteins (1CX2 and 5F1A) studied. The binding sites and interactions from the docking results for COX inhibitors studied in this work are presented in Table S5A-E. Both blind and grid docking studies were carried out and the results for blind docking are given in Table S6. Researchers often use ratios of COX2:COX1 inhibition (Table S7), as most of the cyclox inhibitors are known to inhibit both proteins in different proportions. The molecular docking results suggest that researchers are either overlooking data or abiding by consensus imposed with partial explorations, quite like the cytochrome P450 research field (30, 72). Once again, binding to the active site does not fully explain why or how these inhibitors specifically or preferentially inhibit either COX1 or COX2, or both. More likely, it appears that various molecules could wedge themselves into the narrow channel opening (cyclox-site entry) within the lipid zone, thereby affecting DRS-dynamics. The data also suggests that crystallization of membrane proteins does not give identical structures when carried out with different conditions or by different labs. Also, the murburn postulation of DRS-interactive equilibriums and dynamics thereof could explain the observations obtained.

3.5. Experimental kinetics and stoichiometry profiles:

The complex chemistry of cyclooxygenases has led to several investigations into the structure-function aspects of COX1 and COX2, leading some to propose a reaction network comprising of almost 35 intraenzyme reactions involving 24 different intermediates of the enzyme (73). The K_m , K_{cat} and K_{cat}/K_m values (O_2 consumption) of WT mCOX2 were $4 \mu M$, $55.2 s^{-1}$ and $13.8 \mu M^{-1} s^{-1}$, respectively. Such reaction networks can be confusing and may not be very pragmatic. The murburn model for related heme enzyme like cytochrome P450 has shown that such conventional constants have little practical relevance or utility in understanding the enzyme action.

Reckoning that two O_2 molecules are consumed per fatty acid substrate, at least 27 molecules of AA should be converted per second to PGG₂. Such a high turnover number ($\sim 55 s^{-1}$) and close to 3500 mol of arachidonate/min/mol of dimer for fatty acids (74, 75) is inexplicable because substrate binding & positioning, dynamics within the active site, product formation and finally, product release may not happen at such fast rates. Considering that fatty acids such as AA have a surface area-diffusion profile of $\sim 1 mm^2/s$ (76), the linear mobility is approximately a nanometer within a microsecond. The diffusion restrictions imposed by the catalytic site for the long AA molecule would be significantly higher, by several orders of magnitude. Therefore, the incorporation of AA in some X-ray structures cannot be correlated to physiological realms. Substrates of COX enzymes bind to the same active site pocket in similar fashion and are supposed to get converted by the same mechanistic fashion. Despite this, the catalytic rates (O_2 consumption and substrate oxidation) of both hCOX1 and hCOX2 for AA, EPA, dihomo- γ -linolenate, linoleate, α -linoleate, γ -linoleate, etc. were not the same for 20:4 for both COX1 and COX2 (71). While C20 substrates were found to incorporate 2 moles of O_2 , C18 substrates were found to incorporate only one mole of O_2 per mole of substrate. These aspects of COX kinetics cannot be explained by classical Michaelis-binding based logic.

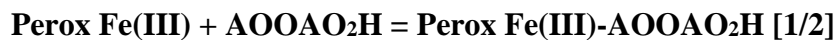
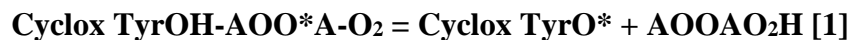
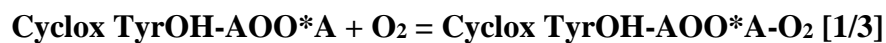
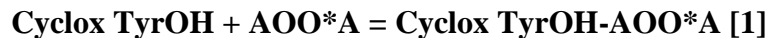
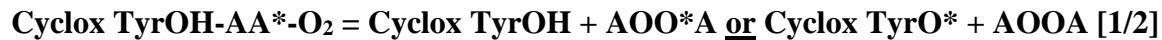
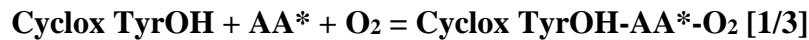
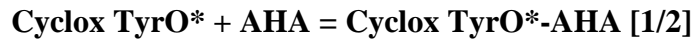
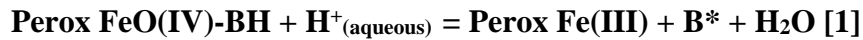
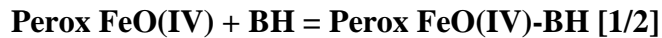
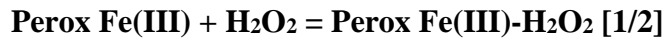
Most importantly, thorough studies on the impact and profiles of molecules on COX activity show tell-tale evidence of the operational relevance of murburn concept. In studies tracing the effect of additives or mutations on COX (45, 77, 78), the activation and inhibition profiles (although plotted with a Michaelis hyperbola fit, e.g. Figure 4 of Rowlinson et al., 2003(78) (for activation) and Figure 2 of Gierse et al., 1996 (45) (for inhibition!) show multi-phasic nature. We have already called out such aspects in the cytochrome P450 murzyme system (17, 29, 30). Also, analysis of

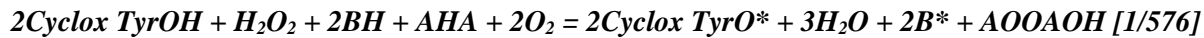
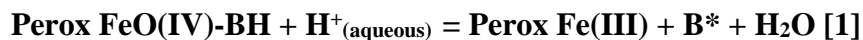
the incubation mixture for products formed clearly shows the non-specific nature of the reaction [Figure 3 of Bai & Zhu, 2008 (77)]. Such experimental findings strongly support the operational relevance of murburn concept in cyclooxygenase function.

3.6. Other miscellaneous supporting arguments for the murburn model of COX:

(1) Several tyrosine residues could be involved in mediating the formation as well as stabilization of DRS generated from heme iron or a fortuitous DRS that could float by could also be stabilised. Moreover, since DRS could be very accessible in the hydrophobic interiors of lipids and protein, they may have ET transducing roles in such realms (22, 79).

(2) The protein structure (cyclox site) does not support an internal migration route for the incomplete product of PGG₂, to move from cyclox-site to perox-site. Hence, PGG₂ formed at the cyclox site would need to detach and move out of the cyclox site, and then into aqueous milieus - and then bind to the perox site. A simple probability assessment (80) of the sequential classical scheme shown in Figures 1 and 2 would be (probability indices given in large braces; arachidonic acid or AA is written here as AHA to enable accounting for hydrogen atom):





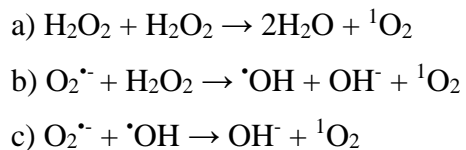
To the best of our knowledge, the overall mass-charge balanced sequential equation of the COX reaction is presented above for the first time. It would need a proton conduit from the cyclox site lipid phase to perox site aqueous phase (which would not permit the tyrosine radical stabilization and catalysis at cyclox site!) AND it also sets off a radical chain reaction in both lipid and aqueous phases! This would mean that one molecule of peroxide would initiate a radical chain reaction that would theoretically give perpetual/endless amount of PGG₂, if oxygen is supplied in plenty. This mechanistic premise does not make physiological sense, and clearly calls out as support for murburn scheme. Quite simply, the mass-charge balanced overall equation and scheme for classical mechanism argues that it cannot be a sole tyrosine-mediated catalysis (like that by Tyr385), but the approximately two-dozen tyrosines on the protein (~3.8% of the amino acid residues, compared to ~2% in various proteins like amylase, lysozyme, collagen, hemoglobin, cytochrome c, etc.) are secondary catalyst/substrate in the DRS-mediated reaction in the vicinity of the heme-Fe enzyme! It can be envisaged that since the phenolic O atom can effectively equilibrate with other O-atom species carrying a 1e surplus/deficiency, nature merely evolved COX with multitudes of DRS-channels and tyrosines to enhance the lifetime of DRS around itself.

(3) DRS produced in cells are known to trigger transcriptional upregulation of COX2 and consequently, higher COX2 activity (81). However, a study showed that DRS formation from COX can increase the enzymatic activity of COX2, without involving higher gene and protein expression of COX2 (82). It also showed that higher ROS-dependent COX activity was the cause of greater pro-oxidant status in aged rats, causing dementia. Many such independent reports connect DRS (and oxidative stress) to greater action of COX enzymes in living cells and tissues. Therefore, cyclooxygenase enzyme action cannot be based just on Michaelis-Menten binding-based approach and would involve the intermediacy of DRS, as numerous reports demonstrate.

Some altogether dismiss the role of DRS in the cyclooxygenase reaction (83), which we believe is based in aesthetic/stigmatic bias. In this connection, evidence was presented to demonstrate that $^1\text{O}_2$ formed from the peroxidase reaction initiates prostaglandin synthesis (84). It is well-known that cyclooxygenases act in tandem with tissue-specific prostaglandin and thromboxin synthases to yield diverse bioactive eicosanoid end-products (85). It was proposed that a singlet oxygen metal complex reacts with unsaturated fatty acid substrate via a peroxidase mechanism, to yield an unconjugated hydroperoxide, which further reacts with the peroxidase part of prostaglandin synthetase complex to form an endoperoxide via a two-step consecutive radical cyclization reaction.

Interestingly, many researchers have shown that singlet oxygen is generated by cyclooxygenases, and that different classes of COX (cyclox site) inhibitors, merely by their virtue of redox activity, are known to react with singlet oxygen, and thus, inhibit AA turnover into PGG₂(86). For example, indole-2 and 3-carboxamides inhibit COX enzymes very efficiently(40); COX enzymes produce DRS such as singlet oxygen & other DRS and most COX inhibitors have antioxidant properties. Ketoprofen and tolmetin are prime examples of NSAIDs with superoxide scavenging activity and thereby, inhibit tissue destruction by DRS and free radicals (87) and these compounds are also scavengers of singlet oxygen. This is why several natural compounds like flavonoids and coumarins inhibit cyclox activity, even though they possess very large surface areas. N-substituted indole-2-carboxylic acid esters were found to scavenge hydroxyl radicals as well as singlet oxygen; thus, a majority of indole esters quenched singlet oxygen directly (in reaction milieu without the involvement of enzyme active site reactions) and thereby exhibited effective antioxidant actions (88). Both redox and non-redox mechanisms (such as redox potential of natural compounds as well as binding affinity) were deemed to contribute to inhibition of COX proteins (89). Novel coumarinyl-1,3,4-oxadiazolyl-2-mercaptopbenzoxazoles with antioxidant activity inhibited both COX1 and COX2 and showed higher selectivity for COX2; these compounds exhibited DPPH radical scavenging activity (90). Indole derivatives were found to scavenge superoxide, hydroxyl radicals as well as singlet oxygen in a concentration-dependent manner, quenching almost 60% of the generated singlet oxygen at 1 mM concentration (40). NSAIDs possess singlet oxygen-scavenging activities, as demonstrated by Costa et al., 2008 (86); singlet oxygen is generated from

a) H₂O₂ disproportionation reactions, b) Haber-Weiss reaction (between H₂O₂ and O₂^{·-}) and c) reaction of radical-radical collapse (O₂^{·-} reaction with ·OH). The above mentioned reactions are given below:



COX enzymes are famously known to generate DRS and are majorly responsible for generation of significant oxidative stress in several maladies (91). Sulindac sulfide is known to be one of the most powerful scavengers of singlet oxygen among the NSAID class (86).

Given the volume of data above (and the literature provided below), it is evident that the scientific community has largely ignored the direct involvement of DRS in the COX system and the DRS-quenching/modulating roles of cyclooxygenase inhibitors. Several fatty acids found in food also have been reported to possess antioxidant and cyclooxygenase-inhibitory activity (92). Numerous natural compounds, which are also well-known for their anti-inflammatory and antioxidant actions have been reported to inhibit cyclooxygenase activity (10). A report suggests that natural compounds are COX1-selective; therefore, functional group modifications were deemed to improve COX2 selectivity of these compounds (93). Also, most of them are known to inhibit either peroxidase and cyclooxygenase (dioxygenation) activities, or both (94). Moreover, antioxidants are known to reduce the gene expression of COX enzymes. For example, epigallocatechin gallate (EGCG) inhibited COX1 more strongly than aspirin at a concentration of 50 Mm (95). Some antioxidant molecules such as EGCG are too large to even enter the cycloxy site, and may still inhibit cycloxy or peroxy activity even if bound to alternative sites on the enzyme. These inhibitors of cyclooxygenases – both natural and synthetic, do not mimic the structure of the fatty acid substrates. From an evolutionary standpoint, it is inconceivable how nature would have selected such structurally dissimilar (to substrate) and diverse inhibitors. Several COX inhibitors have DRS-neutralizing properties and therefore, have beneficial roles against many diseases. Utilization of DRS-suppressing COX inhibitors minimise the damaging side-effects of radiation chemotherapy (96). DRS-mediated PGE₂ production from carbon tetrachloride and diquat was shown to be independent of COX activity, showing that free radicals had a role in generation of this prostaglandin. In biomembranes, Fenton reaction-based lipid peroxidation reactions lead to formation of lipid peroxides. Ex-active site reactions- specifically, autoxidation reactions

(involving initiation, propagation and chain termination) lead to formation of regio- and stereochemical products of both polyunsaturated fatty acids and sterols, causing the formation of cytotoxic cellular products (97). In our earlier reports, we had questioned the application of the Michaelis-Menten paradigm for explaining all aspects of the catalytic repertoire of heme peroxidases and cytochrome P450s and argued that some facets required an extra-active site mechanism. Also, we demonstrated the role of DRS in the modulations (both enhancement and inhibition) of reactions in peroxidases and cytochrome P450s (28, 98, 99). Therefore, it is strongly suggestive that DRS are not merely wasteful products resulting from uncoupling, but are intrinsically involved in the reaction mechanism of murzymes (such as COX).

3.7. Pan-systemic overview & murburn model of COX function

After alignment using ClustalW with default settings, it is clear that the protein is quite conserved between sheep and humans (Figures S4-S6). Except for very minor variations (like presence of a longer N- and C-term region), human COX1 is not very different from sheep COX-1. Human, bovine and ovine COX1 and COX2 sequences have 60% identity and the key active site residues within the cyclox site are quite well conserved. Three COX-1 PDBs sequences (1EBV, 3KK6 and 3N8Z) were compared with human COX1 (6Y3C) sequence. By comparison of different COX1 from the same sources (3 COX1 from sheep, 2 COX2s each from mouse and humans), we obtained different binding results. This strongly suggests what we have been vouching for long – the crystal structures of such murzymes (and especially membranous/membrane-associated proteins) that function via DRS don't necessarily have a high deterministic drive for ensuring structural/topographical conformity. As a result, they give significant variations. Therefore, in such contexts, it is erroneous to overtly stress on topographical features of a given site and connect it with its binding affinity for a given substrate to interpret reaction outcomes. Our finding is further confirmed by the published inhibition binding studies of various CYPs by the same molecules that also critically affect COX proteins. All these issues necessitate a new explicatory paradigm for COX function.

In the CYPs that could get their Fe-center reduced via a superoxide species donating its electron to the solvent accessible thiolate (following which the Fe(II) could bind to molecular oxygen) or a

superoxide generated from reductase could directly access the distal channel and bind to Fe(III). Similarly, in the COX enzyme, electron could come into the system via a peroxide molecule at the peroxy site, or from a superoxide in the cyclooxygenase/perox site. It is proposed herein that the endoperoxide formation results due to singlet oxygen released (by Fe-catalyzed dismutation) at the peroxy-site, which could access the lipid channel of cyclooxygenase-site via internal migration route. Singlet oxygen-mediated formation of lipid hydroperoxides and endoperoxides has been demonstrated in literature (100). The hydroperoxide formation and O-atom removal thereof could occur within the murzone, via the action of other DRS like superoxide. The deterministic classical scheme of a series of sequential steps leading to the formation of PGG₂ at cyclooxygenase site is of low probability, compared to the parallel/stochastic DRS-based murburn model. Also, multiple products are formed from the cyclooxygenase site, and this also advocates for a chaotic, rather than a deterministic process. The stochastic murburn model provides facile and parallel/independent room for recycle in all phases, as shown in Figure 7. Also, the murburn model prioritises upon the nature of reactants and probability of events. Rouzer and Marnett (2020)(12), in their comprehensive review paper on COX enzymes, opined that “*polyunsaturated fatty acids are highly susceptible to nonenzymatic free radical oxygenation due to their readily abstracted H-atoms, which are attached to allylic carbons located between two double bonds. Thus, H-abstraction at C7, C10 or C13 followed by mono-, di- or even tri- oxygenation to yield a wide range of products.*” The literature on COX enzymes is replete with several inferences that point to the contribution of DRS in the cyclooxygenation of lipid substrates. These discordant and inexplicable observations of DRS generation (and the effects of these radicals thereof) are not mere coincidence, but are both plausible and the modus operandi of redox enzymes. Oxidised lipid generation can occur through the action of non-radical DRS like singlet oxygen, HOCl, ozone and other inorganic radical species formed from hydrogen peroxide, superoxide or nitric oxide (101).

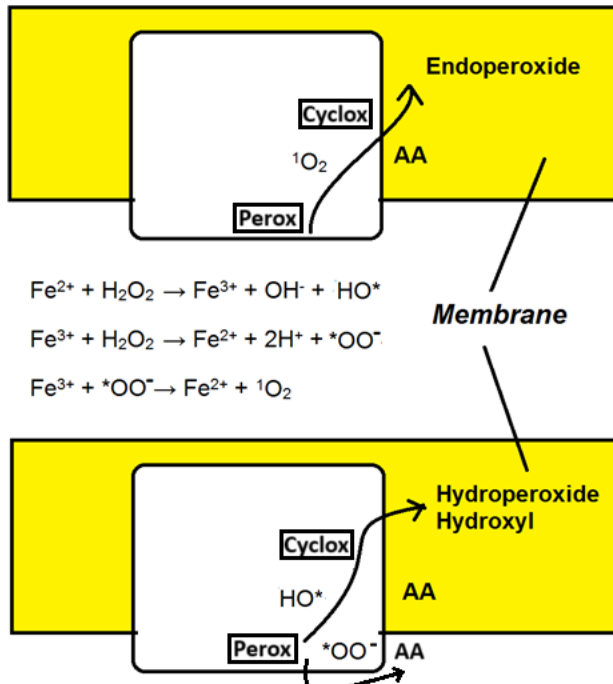


Figure 7: The modality of reaction of various DRS with AA in the murburn model

In Figure 8, comprehensive comparison of the two mechanistic models for overall COX action (involving both the perox and cyclox sites) is depicted. We propose that the murburn model for COX can be ratified by the very same experiments used to demonstrate the murburn model for CYPs. That is: it is predicted that while small amounts of water-soluble antioxidants or DRS-scavenging enzymes would be incapable of causing a major impact on COX-activity, derivatives of the very same species with better hydrophobic positioning would give a greater critical impact. Further, it would be possible to get the formation of PGG₂ starting from arachidonate and COX-membrane system and superoxide.

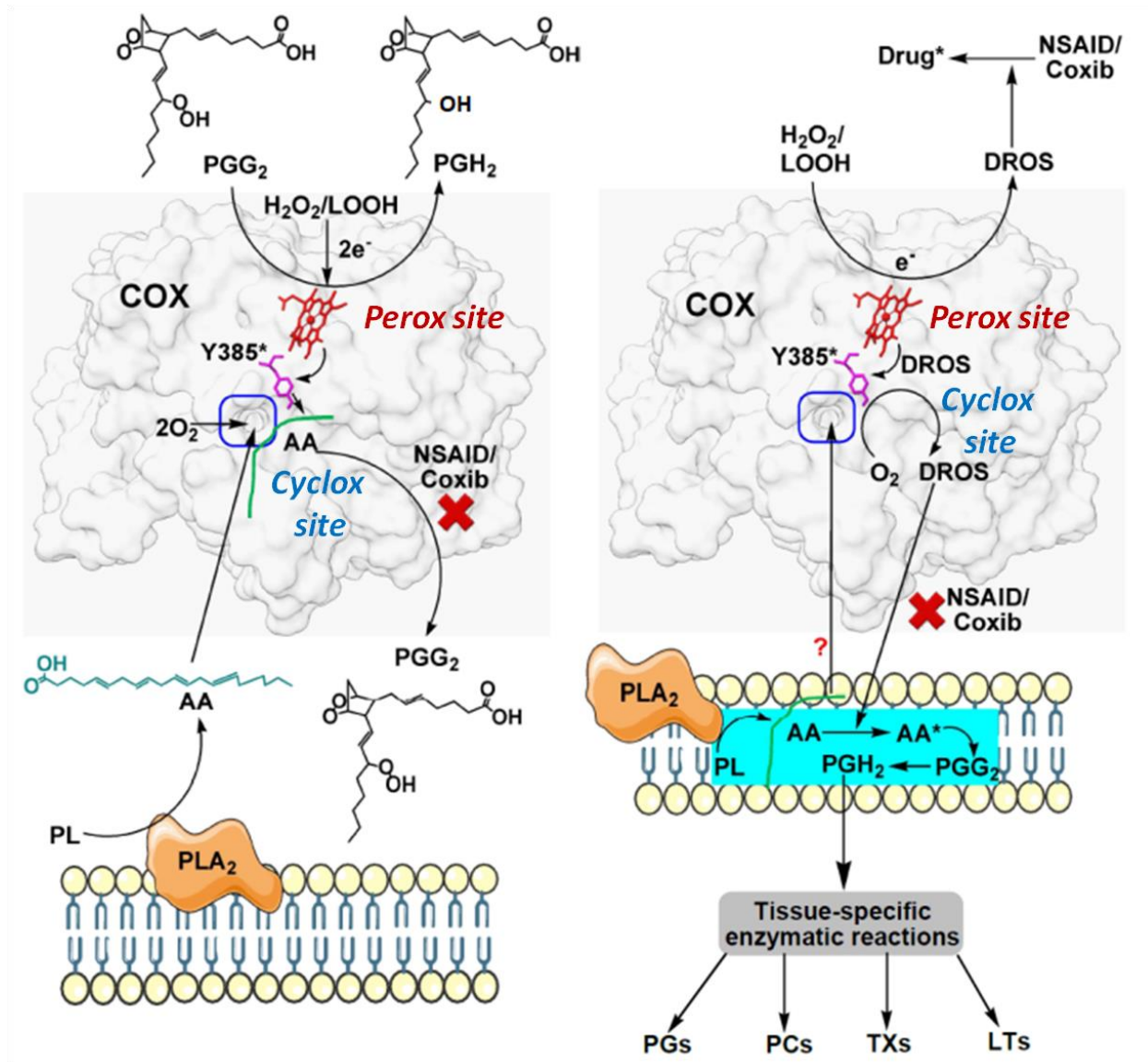


Figure 8: Overall comparison of mechanism of COX action (conventional vs. murburn). The mechanism that is currently widely held is shown to the left. In this mechanism, PLA₂ generates free arachidonic acid (AA) from the membrane, which percolates into the cyclox active site which is placed near the membrane (and faces the membrane). The AA molecule binds in a bent conformation within the narrow active site and a specific carbon atom (C13) is attacked by the tyrosyl radical which is generated by interaction of organic peroxides (LOOH) at the perox site. The oxidant (H_2O_2 /organic peroxide/peroxynitrite) $2e^-$ oxidises heme iron and subsequently, Y385* (tyrosyl radical) generation occurs. The C13 of AA is bound very close to this radical and this enables the attack of the radical on C13, causing C13 to become a carbon-centred radical. An oxygen atom attacks this radical and joins itself to this carbon and later on, a cyclic oxygen ring is formed on AA. Another O_2 atom is attached to AA in the form of OOH and this molecule is called PGG₂. For the reaction to be complete, PGG₂ dissociates from the cyclox site and binds to the peroxidase site and there, it is converted to PGH₂. In the conventional mechanism, AA binding is hampered by the NSAIDs/Coxibs because these drugs block the cyclox site and hence, AA binding and formation of PGG₂ is hampered. In the murburn explanation (shown to the right), there is no absolute necessity for COX enzymes to bind and interact with substrates and inhibitors. Rather, LOOH and peroxide can be converted to form diffusible reduced oxygen species (DROS), which can then attack AA, drugs like NSAIDs and Coxibs and mop up DROS/ROS and thereby, can prevent the formation of PGG₂ and PGH₂. Antioxidants and other cyclox & perox site inhibitors can bind at a favourable

region on the protein in the vicinity of DRS attack and can utilise those DRS and thereby, block both peroxy and cyclooxygenase activities.

4. Conclusions

Herein, we probed the structure-function correlations of a prominent membrane heme-protein, cyclooxygenase. Experts have long strived to arrive at a consensus regarding the inhibition mechanism of COX activity/specificity (6); (However, it has been elusive, as evident from the ongoing efforts which quote varying approaches described in 4 different papers (1, 102-104). The rationale missing was that of ‘murburn’, the novel redox enzyme mechanism that we have been advocating for two decades now, which vouches for the obligatory involvement of DRS in the catalytic mechanism of some redox enzymes, particularly heme enzymes.

1. From a historical perspective (6) and from the current study, it can be discerned that the functional differentiation between COX1 and COX2 are primarily based in the inducibility of expression by glucocorticoids like dexamethasone, and secondarily on the classical active-site mechanistic aspects.
2. In conjunction with the arguments already presented in our earlier work(25), we hereby find that the murburn model for COX is more probable than the classical active-site based mechanism. The cyclooxygenase active site within the membrane phase is too narrow to permit the formation and release of PGG₂; it is merely a DRS channel. The necessity of tyrosine is most likely for enhancing the DRS lifetimes. The data and reasoning trail provided herein are comparable to the one established for CYPs (30, 48), wherein the membrane embedded protein isozymes (as exemplified by CYP3A4, CYP2C9 & CYP2E1) show a number of channels emanating from the distal/proximal site, for facilitating and bringing about effective DRS dynamics and interactions with surface-bound xenobiotic substrates (and these channels are not for substrate access into the occluded and deep-seated heme pocket!).
3. Based on the structural data and probabilistic considerations, we have proposed a testable and facile (in fact, already well supported!) murburn model for the physiological function of the COX enzyme. Biochemical mechanistic insights are best derived from inhibition studies. Our model is

supported and evidenced by the vast numbers and diversity of interfacial redox-active molecules known that could inhibit or/and modulate COX1/2 functions (104): (a) In heterocyclic compounds, the- pyrazole linked thiazoline/benzoxazolone/pyrazoline moieties, (substituted at various 1,2,3,4,5 positions and linked with hydrazone/benzoimidazole/thiourea and benzothiazole, chromenone/acetamide/isothiazole, cinnoline/triazole, isoxazole, oxadiazole, pyrrole and pyrrolidine, substituted phenyl linked thiazolidine, thiazole, thiadiazole, etc.) are classic examples of well-studied class of molecules. Then there are substituted benzoxazoles, substituted isatins, coumarins, indoles, quinolines, isoquinolines, triazoles, tetrazoles, etc., (b) diverse substituted nonheterocyclic compounds, (c) molecular hybrids and fused derivatives, miscellaneous natural products, etc. A look at the diversity of the various molecular structures would convince a discerning individual the explicatory potential of the murburn model for COX. The fact that diverse unsaturated fatty acids are known to serve as substrates for COX is yet another support for the murburn model.

4. The contexts for physiology cannot be justified by a radical propagation in both lipid and aqueous phases. However, it can be well envisaged that disruption of membrane structures would liberate DRS and/or alter DRS dynamics, triggering as an inciting agent for inflammatory response, which is the role perceivable for COX.

5. A DRS like NO is recognised as molecular messenger (105) and exercise (a health promoting activity) is supposed to produce DRS(106). Oxidative stress could also extend life span (107)! ROS are good!! (108). So, it is opportune to rethink the roles of DRS and indulge murburn model of COX, particularly considering that several other heme systems (both soluble and lipid-embedded) have been demonstrated to be murzymes (22).

6. It is well-established that inflammation and immunogenic responses closely tied with COX activity is also intricately connected with observation of DRS and its dynamics thereof. Therefore, considering DRS as a mere artifact in these systems is no more a valid premise and cyclooxygenase should be deemed as a murzyme. Our correlations and inferences drawn herein are capable of qualifying the findings/interpretations of diverse recent works wherein: COX activities are associated with phosphorylations (109), the substrate activity of flurbiprofen for cytochrome

P450s and competitive effects on perox-site in COX (110) can be reasoned, demonstration of interplays of redox active Cu-nanoparticles and COX inhibitors (111), cross-effects of DRS-modulating molecules (e.g., quercetin) and enzymes like iNOS/XO with COX (112, 113), etc.

The new murburn perspectives unraveled herein could enable us to better understand the roles of DRS in immunological and pathophysiological implications of COX enzymes. DRS produced in both healthy and pathophysiological contexts could activate COX (via both perox and cyclox sites, which could turnover diverse substrates in non-specific and non-selective modalities. In this murburn/murzyme schema, diverse additives (like NSAIDS, with high residence times near the enzyme!) could modulate (both activate and inhibit) the enzyme-substrate-DRS interactive dynamics thereby explaining the broad-range of observations, earlier attributed to allosteric binding-induced conformation changes or substrate access alterations to cyclox-site. Isoforms with diversity in surface topography and electrostatics could be affected in distinct ways in such DRS-mediated reactions, thereby addressing the isoform-specific observations, interactions with other proteins and lipids, non-classical metabolites, etc. Since we have already pointed out the Dr. Jekyll and Mr. Hyde persona of DRS, the roles of murzymes in routine health and disease could be re-investigated under this fresh insight. In the larger picture, it is only natural that DRS, which sponsor bioenergetic phosphorylations (powering), fashion redox coherence, homeostasis and mechano-physiological sensing-response facets are ALSO involved in immunological foundations. In toto, it is discernible that murburn concept affords a comprehensive/holistic perspective for integrating various facets and functionalisms of life.

Funding statement

This research did not receive any specific grant from funding agencies in the public, commercial, or not-for-profit sectors.

Declarations

The authors declare that they do not have any conflicts of interest to disclose.

Declaration of generative AI

Statement: During the preparation of this work the author(s) used [ChatGPT] in order to [find out what are the unresolved mysteries in the cyclooxygenase field]. After using this tool/service, the author(s) reviewed and edited the content as needed and take(s) full responsibility for the content of the published article. AI was not used for writing any part of this manuscript.

Author contributions:

DAG and KMM identified crucial shortcomings of the classical explanations and KMM wrote the first draft of the paper, with DAG adding crucial materials and preparing the figures. PA carried out the in silico investigations, prepared tables and presented data. AP analyzed COX structure and provided images/insights.

Conflict of interests: There are no conflicts of interests to declare.

Ethics statement: This article preparation did not involve experimentation with any living systems and the article was prepared along the guidelines provided for authors.

Data availability: All data required to understand and interpret the findings of this work have been duly provided within the manuscript or supplementary information file.

Author CRediT statement

DAG - conceptualization, methodology, validation, visualization, writing - review and editing

PA - Investigation, validation, visualization, software

AP - Investigation, validation, visualization, software

KMM - conceptualization, supervision, validation, writing - original draft, writing - review and editing

Acknowledgments: The work was powered by Satyamjayatu: The Science & Ethics Foundation.

References

1. Blobaum AL, Marnett LJ. Structural and functional basis of cyclooxygenase inhibition. *J Med Chem* 2007; 50(7): 1425-41.
2. Zhao S, Cheng CK, Zhang C-L, Huang Y. Interplay between oxidative stress, cyclooxygenases, and prostanoids in cardiovascular diseases. *Antioxid Redox Signal* 2021; 34(10): 784-99.
3. Sheng J, Sun H, Yu F-B, Li B, Zhang Y, Zhu Y-T. The role of cyclooxygenase-2 in colorectal cancer. *Int J Med Sci* 2020; 17(8): 1095.
4. Rieger JM, Shah AR, Gidday JM. Ischemia-reperfusion injury of retinal endothelium by cyclooxygenase-and xanthine oxidase-derived superoxide. *Exp Eye Res* 2002; 74(4): 493-501.
5. Hla T, Bishop-Bailey D, Liu C, Schaefers H, Trifan OC. Cyclooxygenase-1 and-2 isoforms. *Int J Biochem Cell Biol* 1999; 31(5): 551-7.
6. Brooks P, Emery P, Evans J, Fenner H, Hawkey C, Patrono C, et al. Interpreting the clinical significance of the differential inhibition of cyclooxygenase-1 and cyclooxygenase-2. *Rheumatology* 1999; 38(8): 779-88.
7. Zidar N, Odar K, Glavac D, Jerse M, Zupanc T, Stajer D. Cyclooxygenase in normal human tissues—is COX-1 really a constitutive isoform, and COX-2 an inducible isoform? *J Cell Mol Med* 2009; 13(9b): 3753-63.
8. Smith WL, Langenbach R. Why there are two cyclooxygenase isozymes. *J Clin Invest* 2001; 107(12): 1491-5.
9. Simmons DL, Botting RM, Hla T. Cyclooxygenase isozymes: the biology of prostaglandin synthesis and inhibition. *Pharmacol Rev* 2004; 56(3): 387-437.
10. Chandel P, Rawal RK, Kaur R. Natural products and their derivatives as cyclooxygenase-2 inhibitors. *Future Med Chem* 2018; 10(20): 2471-92.
11. Rouzer CA, Marnett LJ. Cyclooxygenases: structural and functional insights. *J Lipid Res* 2009; 50: S29-S34.
12. Rouzer CA, Marnett LJ. Structural and chemical biology of the interaction of cyclooxygenase with substrates and non-steroidal anti-inflammatory drugs. *Chem Rev* 2020; 120(15): 7592-641.
13. Dailley OD, Wang X, Chen F, Huang G. Anticancer activity of branched-chain derivatives of oleic acid. *Anticancer Res* 2011; 31(10): 3165-9.
14. Yang C, Li P, Ding X, Sui HC, Rao S, Hsu C-H, et al. Mechanism for the reactivation of the peroxidase activity of human cyclooxygenases: investigation using phenol as a reducing cosubstrate. *Sci Rep* 2020; 10(1): 15187.
15. Manoj KM. Murburn posttranslational modifications of proteins: Cellular redox processes and murzyme-mediated metabolo-proteomics. *J Cell Physiol* 2024; 239(3): e30954.
16. Manoj KM, Jaeken L. Synthesis of theories on cellular powering, coherence, homeostasis and electro-mechanics: Murburn concept and evolutionary perspectives. *J Cell Physiol* 2023; 238(5): 931-53.
17. Manoj KM, Baburaj A, Ephraim B, Pappachan F, Maviliparambathu PP, Vijayan UK, et al. Explaining the atypical reaction profiles of heme enzymes with a novel mechanistic hypothesis and kinetic treatment. *PLoS One* 2010; 5(5): e10601.
18. Parashar A, Jacob VD, Gideon DA, Manoj KM. Hemoglobin catalyzes ATP-synthesis in human erythrocytes: a murburn model. *J Biomol Struct Dyn* 2022; 40(19): 8783-95.

19. Manoj KM, Gideon DA, Jaeken L. Interaction of membrane-embedded cytochrome b-complexes with quinols: Classical Q-cycle and murburn model. *Cell Biochem Funct* 2022; 40(2): 118-26.
20. Manoj KM, Nirusimhan V, Parashar A, Edward J, Gideon DA. Murburn precepts for lactic-acidosis, Cori cycle, and Warburg effect: Interactive dynamics of dehydrogenases, protons, and oxygen. *J Cell Physiol* 2022; 237(3): 1902-22.
21. Manoj KM, Gideon DA, Bazhin NM, Tamagawa H, Nirusimhan V, Kavdia M, et al. Na, K-ATPase: A murzyme facilitating thermodynamic equilibriums at the membrane-interface. *J Cell Physiol* 2022.
22. Manoj KM, Gideon DA. Structural foundations for explaining the physiological roles of murzymes embedded in diverse phospholipid membranes. *Biochim Biophys Acta Biomembr* 2022; 1864(10): 183981.
23. Manoj KM, Jaeken L, Bazhin NM, Tamagawa H, Kavdia M, Manekkathodi A. Murburn concept in cellular function and bioenergetics, Part 1: Understanding murzymes at the molecular level. *AIP Adv* 2023; 13(12).
24. Manoj KM, Jaeken L, Bazhin NM, Tamagawa H, Gideon DA, Kavdia M. Murburn concept in cellular function and bioenergetics, Part 2: Understanding integrations-translations from molecular to macroscopic levels. *AIP Adv* 2023; 13(12).
25. Gideon DA, Parashar A, Robin J, Annadurai P, Nirusimhan V, Manoj KM. Do cyclooxygenases possess a murzyme activity? *Biomed Rev* 2021; 32: 47-59.
26. Yang H, Lou C, Sun L, Li J, Cai Y, Wang Z, et al. admetSAR 2.0: web-service for prediction and optimization of chemical ADMET properties. *Bioinformatics* 2019; 35(6): 1067-9.
27. Morris GM, Huey R, Olson AJ. Using autodock for ligand-receptor docking. *Curr Protoc Bioinformatics* 2008; 24(1): 8.14.1-8.40.
28. Manoj KM, Parashar A, Venkatachalam A, Goyal S, Singh PG, Gade SK, et al. Atypical profiles and modulations of heme-enzymes catalyzed outcomes by low amounts of diverse additives suggest diffusible radicals' obligatory involvement in such redox reactions. *Biochimie* 2016; 125: 91-111.
29. Parashar A, Gade SK, Potnuru M, Madhavan N, Manoj KM. The curious case of benzboromarone: insight into super-inhibition of cytochrome P450. *PLoS One* 2014; 9(3): e89967.
30. Manoj KM, Parashar A, Gade SK, Venkatachalam A. Functioning of microsomal cytochrome P450s: Murburn concept explains the metabolism of xenobiotics in hepatocytes. *Front Pharmacol* 2016; 7: 161.
31. Marnett LJ, Rowlinson SW, Goodwin DC, Kalgutkar AS, Lanzo CA. Arachidonic acid oxygenation by COX-1 and COX-2: mechanisms of catalysis and inhibition. *J Biol Chem* 1999; 274(33): 22903-6.
32. Smith WL, Urade Y, Jakobsson P-J. Enzymes of the cyclooxygenase pathways of prostanoïd biosynthesis. *Chem Rev* 2011; 111(10): 5821-65.
33. Patrignani P, Patrono C. Cyclooxygenase inhibitors: from pharmacology to clinical read-outs. *Biochim Biophys Acta Mol Cell Biol Lipids* 2015; 1851(4): 422-32.
34. Van der Donk WA, Tsai A-L, Kulmacz RJ. The cyclooxygenase reaction mechanism. *Biochemistry* 2002; 41(52): 15451-8.
35. Vecchio AJ, Simmons DM, Malkowski MG. Structural basis of fatty acid substrate binding to cyclooxygenase-2. *J Biol Chem* 2010; 285(29): 22152-63.

36. Yuan C, Sidhu RS, Kuklev DV, Kado Y, Wada M, Song I, et al. Cyclooxygenase allosterism, fatty acid-mediated cross-talk between monomers of cyclooxygenase homodimers. *J Biol Chem* 2009; 284(15): 10046-55.
37. Luong C, Miller A, Barnett J, Chow J, Ramesha C, Browner MF. Flexibility of the NSAID binding site in the structure of human cyclooxygenase-2. *Nat Struct Biol* 1996; 3(11): 927-33.
38. Smith WL, Song I. The enzymology of prostaglandin endoperoxide H synthases-1 and-2. *Prostaglandins Other Lipid Mediat* 2002; 68: 115-28.
39. Sono M, Roach MP, Coulter ED, Dawson JH. Heme-containing oxygenases. *Chem Rev* 1996; 96(7): 2841-88.
40. Aboul-Enein HY, Kruk I, Lichszeld K, Michalska T, Kladna A, Marcynski S, et al. Scavenging of reactive oxygen species by N-substituted indole-2 and 3-carboxamides. *Luminescence* 2004; 19(1): 1-7.
41. Rowlinson SW, Crews BC, Lanzo CA, Marnett LJ. The binding of arachidonic acid in the cyclooxygenase active site of mouse prostaglandin endoperoxide synthase-2 (COX-2): a putative L-shaped binding conformation utilizing the top channel region. *J Biol Chem* 1999; 274(33): 23305-10.
42. Lucido MJ, Orlando BJ, Vecchio AJ, Malkowski MG. Crystal structure of aspirin-acetylated human cyclooxygenase-2: insight into the formation of products with reversed stereochemistry. *Biochemistry* 2016; 55(8): 1226-38.
43. Saeed S, Mesaik M, Quadri J, Tasneem S, Motiwala A, Khalid U, et al. Interactions of cyclooxygenase inhibitors with reactive oxygen species. *J Pharmacol Toxicol* 2006; 1(2): 115-25.
44. Zarghi A, Arfaei S. Selective COX-2 inhibitors: a review of their structure-activity relationships. *Iran J Pharm Res* 2011; 10(4): 655.
45. Gierse JK, McDonald JJ, Hauser SD, Rangwala SH, Koboldt CM, Seibert K. A single amino acid difference between cyclooxygenase-1 (COX-1) and- 2 (COX-2) reverses the selectivity of COX-2 specific inhibitors. *J Biol Chem* 1996; 271(26): 15810-4.
46. Fitzpatrick F, Ennis M, Baze M, Wynalda M, McGee J, Liggett W. Inhibition of cyclooxygenase activity and platelet aggregation by epoxyeicosatrienoic acids. Influence of stereochemistry. *J Biol Chem* 1986; 261(32): 15334-8.
47. Huff RG, Bayram E, Tan H, Knutson ST, Knaggs MH, Richon AB, et al. Chemical and structural diversity in cyclooxygenase protein active sites. *Chem Biodivers* 2005; 2(11): 1533-52.
48. Parashar A, Manoj KM. Murburn precepts for cytochrome P450 mediated drug/xenobiotic metabolism and homeostasis. *Curr Drug Metab* 2021; 22(4): 315-26.
49. Cong Y-S, Wright WE, Shay JW. Human telomerase and its regulation. *Microbiol Mol Biol Rev* 2002; 66(3): 407-25.
50. Levin G, Duffin KL, Obukowicz MG, Hummert SL, Fujiwara H, Needleman P, et al. Differential metabolism of dihomo- γ -linolenic acid and arachidonic acid by cyclo-oxygenase-1 and cyclo-oxygenase-2: implications for cellular synthesis of prostaglandin E1 and prostaglandin E2. *Biochem J* 2002; 365(2): 489-96.
51. Campbell WB, Falck JR, Okita JR, Johnson AR, Callahan KS. Synthesis of dihomoprostaglandins from adrenic acid (7, 10, 13, 16-docosatetraenoic acid) by human endothelial cells. *Biochim Biophys Acta Lipids Lipid Metab* 1985; 837(1): 67-76.

52. Mann CJ, Kaduce TL, Figard PH, Spector AA. Docosatetraenoic acid in endothelial cells: formation, retroconversion to arachidonic acid, and effect on prostacyclin production. *Arch Biochem Biophys* 1986; 244(2): 813-23.
53. Malkowski MG, Thuresson ED, Lakkides KM, Rieke CJ, Micielli R, Smith WL, et al. Structure of eicosapentaenoic and linoleic acids in the cyclooxygenase site of prostaglandin endoperoxide H synthase-1. *J Biol Chem* 2001; 276(40): 37547-55.
54. Dong L, Zou H, Yuan C, Hong YH, Kuklev DV, Smith WL. Different fatty acids compete with arachidonic acid for binding to the allosteric or catalytic subunits of cyclooxygenases to regulate prostanoid synthesis. *J Biol Chem* 2016; 291(8): 4069-78.
55. Shimokawa T, Kulmacz RJ, Dewitt DL, Smith WL. Tyrosine 385 of prostaglandin endoperoxide synthase is required for cyclooxygenase catalysis. *J Biol Chem* 1990; 265(33): 20073-6.
56. Tsai A-L, Hsi LC, Kulmacz RJ, Palmer G, Smith WL. Characterization of the tyrosyl radicals in ovine prostaglandin H synthase-1 by isotope replacement and site-directed mutagenesis. *J Biol Chem* 1994; 269(7): 5085-91.
57. Wu G, Tsai A-L, Kulmacz RJ. Cyclooxygenase competitive inhibitors alter tyrosyl radical dynamics in prostaglandin H synthase-2. *Biochemistry* 2009; 48(50): 11902-11.
58. Bhattacharyya DK, Lecomte M, Rieke CJ, Garavito RM, Smith WL. Involvement of arginine 120, glutamate 524, and tyrosine 355 in the binding of arachidonate and 2-phenylpropionic acid inhibitors to the cyclooxygenase active site of ovine prostaglandin endoperoxide H synthase-1. *J Biol Chem* 1996; 271(4): 2179-84.
59. Rieke CJ, Mulichak AM, Garavito RM, Smith WL. The role of arginine 120 of human prostaglandin endoperoxide H synthase-2 in the interaction with fatty acid substrates and inhibitors. *J Biol Chem* 1999; 274(24): 17109-14.
60. Konkle ME, Blobaum AL, Moth CW, Prusakiewicz JJ, Xu S, Ghebreselasie K, et al. Conservative secondary shell substitution in cyclooxygenase-2 reduces inhibition by indomethacin amides and esters via altered enzyme dynamics. *Biochemistry* 2016; 55(2): 348-59.
61. Blobaum AL, Xu S, Rowlinson SW, Duggan KC, Banerjee S, Kudalkar SN, et al. Action at a distance: mutations of peripheral residues transform rapid reversible inhibitors to slow, tight binders of cyclooxygenase-2. *J Biol Chem* 2015; 290(20): 12793-803.
62. Kurumbail RG, Stevens AM, Gierse JK, McDonald JJ, Stegeman RA, Pak JY, et al. Structural basis for selective inhibition of cyclooxygenase-2 by anti-inflammatory agents. *Nature* 1996; 384(6610): 644-8.
63. Viegas A, Manso J, Corvo MC, Marques MMB, Cabrita EJ. Binding of ibuprofen, ketorolac, and diclofenac to COX-1 and COX-2 studied by saturation transfer difference NMR. *J Med Chem* 2011; 54(24): 8555-62.
64. Stevens AM, Pawlitz JL, Kurumbail RG, Gierse JK, Moreland KT, Stegeman RA, et al. Crystallization of recombinant cyclo-oxygenase-2. *J Cryst Growth* 1999; 196(2-4): 350-5.
65. Schneider C, Boeglin WE, Brash AR. Identification of two cyclooxygenase active site residues, leucine 384 and glycine 526, that control carbon ring cyclization in prostaglandin biosynthesis. *J Biol Chem* 2004; 279(6): 4404-14.

66. Sevigny MB, Li C-F, Alas M, Hughes-Fulford M. Glycosylation regulates turnover of cyclooxygenase-2. *FEBS Lett* 2006; 580(28-29): 6533-6.
67. Sevigny MB, Graham K, Ponce E, Louie MC, Mitchell K. Glycosylation of human cyclooxygenase-2 (COX-2) decreases the efficacy of certain COX-2 inhibitors. *Pharmacol Res* 2012; 65(4): 445-50.
68. Yap YH-Y, Say Y-H. Resistance against apoptosis by the cellular prion protein is dependent on its glycosylation status in oral HSC-2 and colon LS 174T cancer cells. *Cancer Lett* 2011; 306(1): 111-9.
69. Greig GM, Francis DA, Falgueyret J-P, Ouellet M, Percival MD, Roy P, et al. The interaction of arginine 106 of human prostaglandin G/H synthase-2 with inhibitors is not a universal component of inhibition mediated by nonsteroidal anti-inflammatory drugs. *Mol Pharmacol* 1997; 52(5): 829-38.
70. Levoine N, Blondeau C, Guillaume C, Grandcolas L, Chretien F, Jouzeau J-Y, et al. Elucidation of the mechanism of inhibition of cyclooxygenases by acyl-coenzyme A and acylglucuronic conjugates of ketoprofen. *Biochem Pharmacol* 2004; 68(10): 1957-69.
71. Laneuville O, Breuer DK, Xu N, Huang Z, Gage DA, Watson JT, et al. Fatty acid substrate specificities of human prostaglandin-endoperoxide H synthase-1 and- 2: formation of 12-hydroxy-(9Z, 13E/Z, 15Z)-octadecatrienoic acids from α -linolenic acid. *J Biol Chem* 1995; 270(33): 19330-6.
72. Venkatachalam A, Parashar A, Manoj KM. Functioning of drug-metabolizing microsomal cytochrome P450s: in silico probing of proteins suggests that the distal heme ‘active site’ pocket plays a relatively ‘passive role’ in some enzyme-substrate interactions. *In Silico Pharmacol* 2016; 4: 1-38.
73. Goltsov A, Swat M, Peskov K, Kosinsky Y. Cycle network model of prostaglandin H synthase-1. *Pharmaceuticals* 2020; 13(10): 265.
74. Thuresson ED, Lakkides KM, Smith WL. Different catalytically competent arrangements of arachidonic acid within the cyclooxygenase active site of prostaglandin endoperoxide H synthase-1 lead to the formation of different oxygenated products. *J Biol Chem* 2000; 275(12): 8501-7.
75. Wu G, Lü J-M, Van Der Donk WA, Kulmacz RJ, Tsai A-L. Cyclooxygenase reaction mechanism of prostaglandin H synthase from deuterium kinetic isotope effects. *J Inorg Biochem* 2011; 105(3): 382-90.
76. Moltu SJ, Nordvik T, Rossholt ME, Wendel K, Chawla M, Server A, et al. Arachidonic and docosahexaenoic acid supplementation and brain maturation in preterm infants: a double blind RCT. *Clin Nutr* 2024; 43(1): 176-86.
77. Bai H-W, Zhu BT. Strong activation of cyclooxygenase I and II catalytic activity by dietary bioflavonoids. *J Lipid Res* 2008; 49(12): 2557-70.
78. Rowlinson SW, Kiefer JR, Prusakiewicz JJ, Pawlitz JL, Kozak KR, Kalgutkar AS, et al. A novel mechanism of cyclooxygenase-2 inhibition involving interactions with Ser-530 and Tyr-385. *J Biol Chem* 2003; 278(46): 45763-9.
79. Gideon DA, Nirushan V, E JC, Sudarsha K, Manoj KM. Mechanism of electron transfers mediated by cytochromes c and b 5 in mitochondria and endoplasmic reticulum: classical and murburn perspectives. *J Biomol Struct Dyn* 2022; 40(19): 9235-52.

80. Manoj KM, Gideon DA, Parashar A. What is the role of lipid membrane-embedded quinones in mitochondria and chloroplasts? Chemiosmotic Q-cycle versus murburn reaction perspective. *Cell Biochem Biophys* 2021; 79(1): 3-10.
81. Barbieri SS, Eligini S, Brambilla M, Tremoli E, Colli S. Reactive oxygen species mediate cyclooxygenase-2 induction during monocyte to macrophage differentiation: critical role of NADPH oxidase. *Cardiovasc Res* 2003; 60(1): 187-97.
82. Baek BS, Kim JW, Lee JH, Kwon HJ, Kim ND, Kang HS, et al. Age-related increase of brain cyclooxygenase activity and dietary modulation of oxidative status. *J Gerontol A Biol Sci Med Sci* 2001; 56(10): B426-B31.
83. Baumann J, Wurm G. Studies on the possible involvement of singlet oxygen and superoxide anion radicals in the cyclo-oxygenase reaction. *Prostaglandins Leukot Med* 1984; 14(1): 139-52.
84. Rahimtula A, O'Brien PJ. The possible involvement of singlet oxygen in prostaglandin biosynthesis. *Biochem Biophys Res Commun* 1976; 70(3): 893-9.
85. Tanabe T, Ullrich V. Prostacyclin and thromboxane synthases. *J Lipid Mediat Cell Signal* 1995; 12(2-3): 243-55.
86. Costa D, Gomes A, Lima JL, Fernandes E. Singlet oxygen scavenging activity of non-steroidal anti-inflammatory drugs. *Redox Rep* 2008; 13(4): 153-60.
87. Kładna A, Aboul-Enein HY, Kruk I, Lichszeld K, Michalska T. Scavenging of reactive oxygen species by some nonsteroidal anti-inflammatory drugs and fenofibrate. *Biopolymers* 2006; 82(2): 99-105.
88. Kruk I, Aboul-Enein HY, Michalska T, Lichszeld K, Kubasik-Kładna K, Ölgen S. In vitro scavenging activity for reactive oxygen species by N-substituted indole-2-carboxylic acid esters. *Luminescence* 2007; 22(4): 379-86.
89. Landa P, Kutil Z, Temml V, Vuorinen A, Malik J, Dvorakova M, et al. Redox and non-redox mechanism of in vitro cyclooxygenase inhibition by natural quinones. *Planta Med* 2012; 78(04): 326-33.
90. Nesaragi AR, Kamble RR, Dixit S, Kodasi B, Hoolageri SR, Bayannavar PK, et al. Green synthesis of therapeutically active 1, 3, 4-oxadiazoles as antioxidants, selective COX-2 inhibitors and their in silico studies. *Bioorg Med Chem Lett* 2021; 43: 128112.
91. Villegas I, Martín M, La Casa C, Motilva V, Alarcón De La Lastra C. Effects of oxicam inhibitors of cyclooxygenase on oxidative stress generation in rat gastric mucosa: A comparative study. *Free Radic Res* 2002; 36(7): 769-77.
92. Henry GE, Momin RA, Nair MG, Dewitt DL. Antioxidant and cyclooxygenase activities of fatty acids found in food. *J Agric Food Chem* 2002; 50(8): 2231-4.
93. Jachak SM. Cyclooxygenase inhibitory natural products: current status. *Curr Med Chem* 2006; 13(6): 659-78.
94. Amessis-Ouchemoukh N, Madani K, Falé PL, Serralheiro ML, Araújo MEM. Antioxidant capacity and phenolic contents of some Mediterranean medicinal plants and their potential role in the inhibition of cyclooxygenase-1 and acetylcholinesterase activities. *Ind Crops Prod* 2014; 53: 6-15.
95. Lee D-H, Kim Y-J, Kim H-H, Cho H-J, Ryu J-H, Rhee MH, et al. Inhibitory effects of epigallocatechin-3-gallate on microsomal cyclooxygenase-1 activity in platelets. *Biomolecules Ther* 2013; 21(1): 54.

96. Laube M, Kniess T, Pietzsch J. Development of antioxidant COX-2 inhibitors as radioprotective agents for radiation therapy: A hypothesis-driven review. *Antioxidants* 2016; 5(2): 14.
97. Zielinski ZA, Pratt DA. Lipid peroxidation: kinetics, mechanisms, and products. *J Org Chem* 2017; 82(6): 2817-25.
98. Andrew D, Hager L, Manoj KM. The intriguing enhancement of chloroperoxidase mediated one-electron oxidations by azide, a known active-site ligand. *Biochem Biophys Res Commun* 2011; 415(4): 646-9.
99. Parashar A, Manoj KM. Traces of certain drug molecules can enhance heme-enzyme catalytic outcomes. *Biochem Biophys Res Commun* 2012; 417(3): 1041-5.
100. Pryor WA, Houk KN, Foote CS, Fukuto JM, Ignarro LJ, Squadrito GL, Davies KJA. Free radicals in biology and medicine: From basic science to health implications. *Am J Physiol Regul Integr Comp Physiol* 2006; 291: R491-R511.
101. Smith WL, Murphy RC. Oxidized lipids formed non-enzymatically by reactive oxygen species. *J Biol Chem* 2008; 283(23): 15513-4.
102. Kaur M, Kaur B, Kaur J, Kaur A, Bhatti R, Singh P. Role of water in cyclooxygenase catalysis and design of anti-inflammatory agents targeting two sites of the enzyme. *Sci Rep* 2020; 10(1): 10764.
103. Ju Z, Li M, Xu J, Howell DC, Li Z, Chen F-E. Recent development on COX-2 inhibitors as promising anti-inflammatory agents: The past 10 years. *Acta Pharm Sin B* 2022; 12(6): 2790-807.
104. Chahal S, Rani P, Kiran, Sindhu J, Joshi G, Ganesan A, et al. Design and development of COX-II inhibitors: Current scenario and future perspective. *ACS Omega* 2023; 8(20): 17446-98.
105. Ignarro LJ, Cirino G, Casini A, Napoli C. Nitric oxide as a signaling molecule in the vascular system: An overview. *J Cardiovasc Pharmacol* 1999; 34(6): 879-86.
106. Powers SK, Nelson WB, Hudson MB. Exercise-induced oxidative stress in humans: cause and consequences. *Free Radic Biol Med* 2011; 51(5): 942-50.
107. Ristow M, Schmeisser S. Extending life span by increasing oxidative stress. *Free Radic Biol Med* 2011; 51(2): 327-36.
108. Mittler R. ROS are good. *Trends Plant Sci* 2017; 22(1): 11-9.
109. Hussain S, Iqbal A, Hamid S, Putra PP, Ashraf M. Identifying alkaline phosphatase inhibitory potential of cyclooxygenase-2 inhibitors: Insights from molecular docking, MD simulations, molecular expression analysis in MCF-7 breast cancer cell line and in vitro investigations. *Int J Biol Macromol* 2024; 132: 721.
110. Alam A, Ali M, Rehman NU, Latif A, Shah AJ, Wazir NU, et al. Synthesis and characterization of biologically active flurbiprofen amide derivatives as selective prostaglandin-endoperoxide synthase II inhibitors: In vivo anti-inflammatory activity and molecular docking. *Int J Biol Macromol* 2023; 228: 659-70.
111. Elmehbad NY, Mohamed NA, Abd El-Ghany NA, Abdel-Aziz MM. Evaluation of the in vitro anti-inflammatory and anti-Helicobacter pylori activities of chitosan-based biomaterials modified with copper oxide nanoparticles. *Int J Biol Macromol* 2023; 253: 127277.
112. Mukherjee D, Ahmad R, Nayeem S. Molecular interplay promotes amelioration by quercetin during experimental hepatic inflammation in rodents. *Int J Biol Macromol* 2022; 222: 2936-47.

113. Zhou H, Feng L, Weng X, Wang T, Lu H, Bian Y, et al. Inhibition mechanism of cordycepin and ergosterol from *Cordyceps militaris* Link. against xanthine oxidase and cyclooxygenase-2. *Int J Biol Macromol* 2024; 258: 128898.

SUPPLEMENTARY INFORMATION

Re-interpretation of structure-function correlations and inhibitions of mammalian cyclooxygenase isozymes with murburn concept

Daniel Andrew Gideon¹, Pushparaj Annadurai², Abhinav Parashar³, Kelath Murali Manoj^{4,5*}*

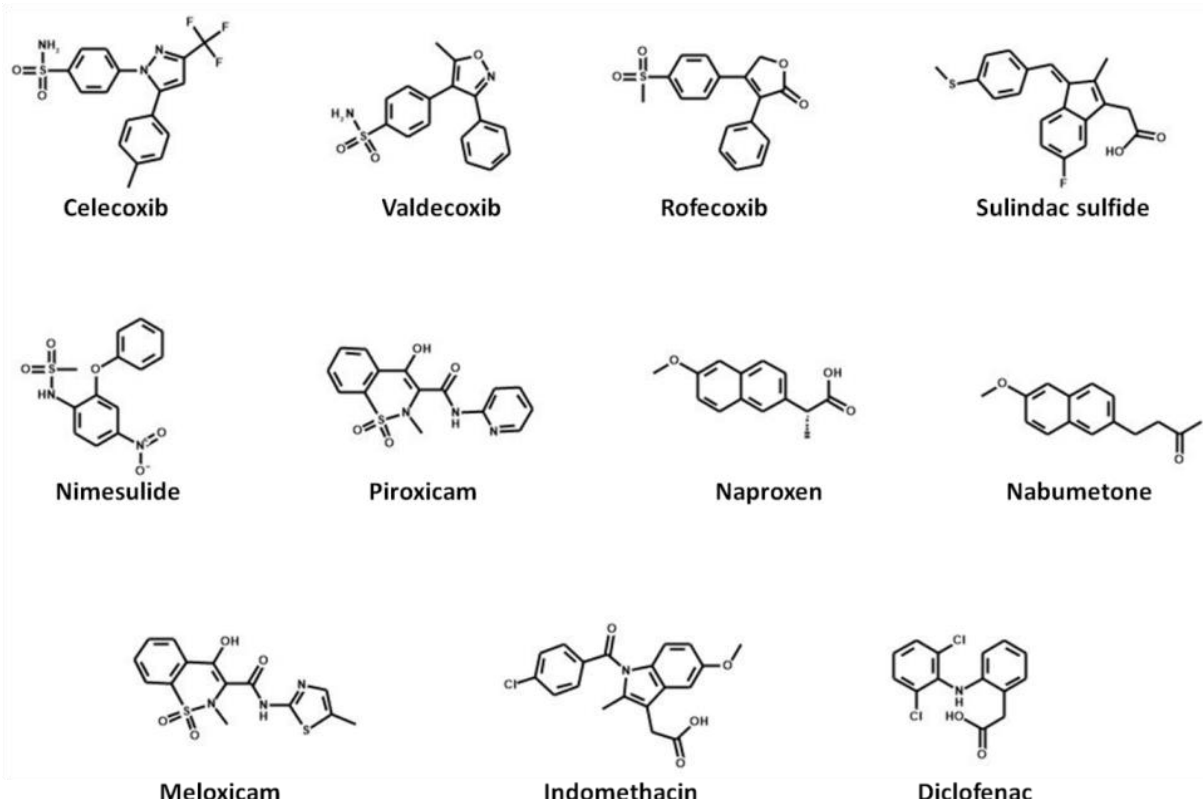


Figure S1: Molecular structures of inhibitors chosen as ligands for blind and grid-centered docking studies

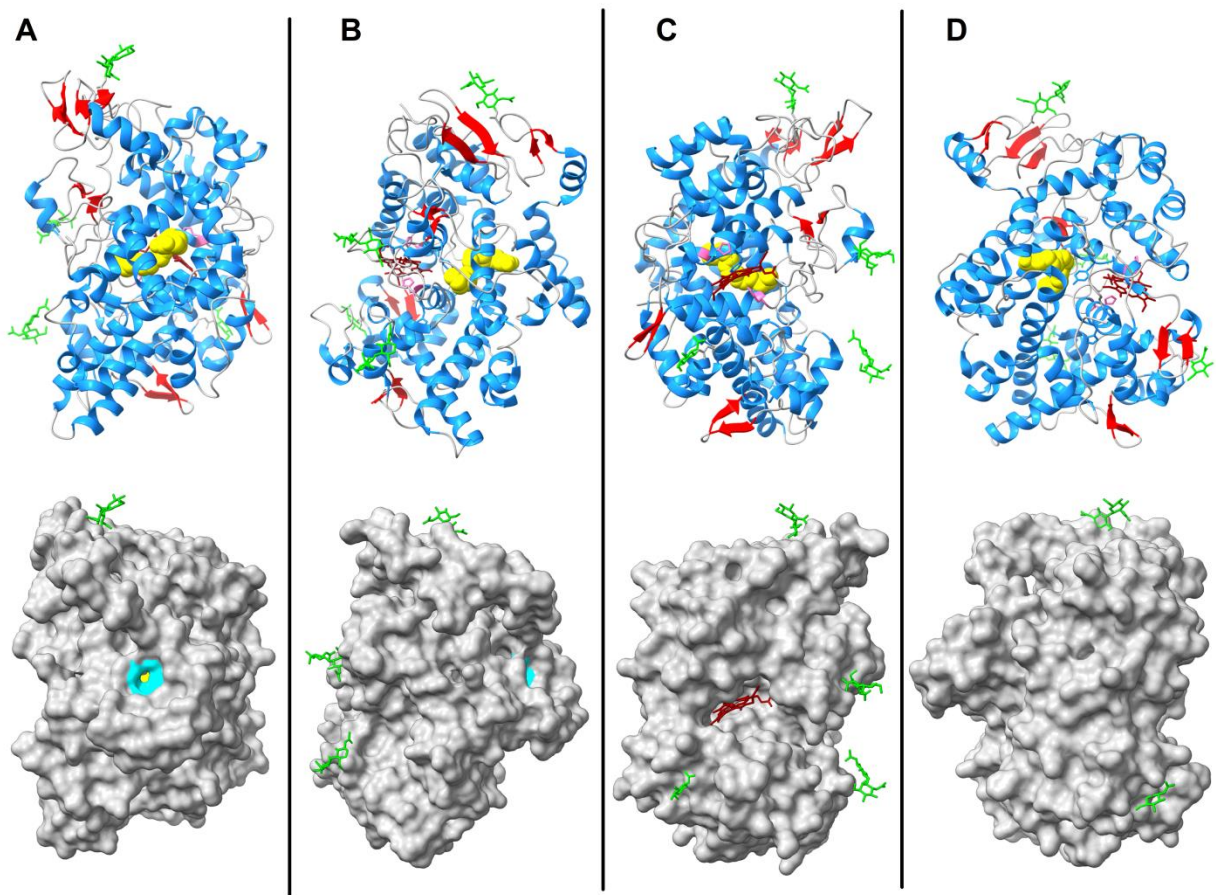


Figure S2. Overview of mCOX2 (PDB ID: 3HS5): Panels A-D (separated by a black line) show the respective tertiary structure poses of the protein on the top side of each panel and the corresponding surface views at the bottom side of each panel. The poses in each panel are almost 90° left in each panel (from A to D). All secondary structures are coloured as follows: alpha helices are blue, beta sheets are red, and random coils are grey. The heme-coordinating His residues are coloured pink. The glycans are coloured as green sticks and heme is coloured as brownish red stick. The extreme left panel (A) shows the membrane side of mCOX2 monomer; AA is coloured as yellow spheres, with the cycloox entry channel residues' surfaces in cyan (bottom Figure of panel A). The heme binding perox site (seen in panel C) is almost on the opposite side of the cycloox entry channel (panel A).

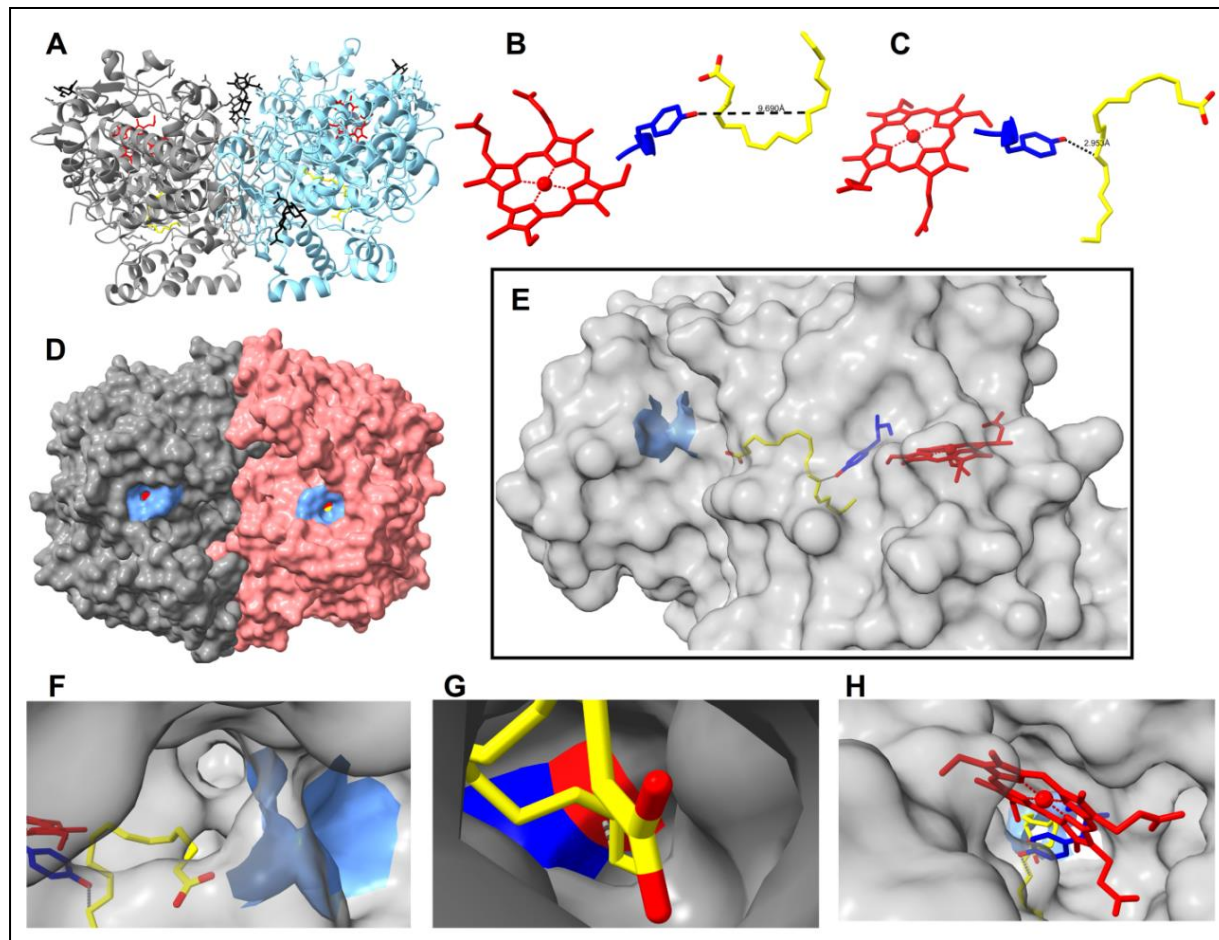


Figure S3: Insight into various structural aspects of COX enzymes. *mCOX2 dimer showing the overview of the protein. In this crystal structure (3HS5), AA binding in two different monomers differs significantly. Heme residues are shown in red and AA is shown as yellow stick. Glycans are coloured black. In chain A (gray colouring in panel A), AA was found to bind non-productively, with the C13 of AA nearly 10 Å away from the OH group of Y385 (shown in panel B). In panel C, the productive binding of AA was discovered with COOH end of AA located near the cycloox active site entry channel and in this case, Y385 OH group was nearly 3 Å away from C13 of AA (panel C), where the Y385* attack on AA is understood to occur. Thus, to two different monomers of the same protein, AA binding has been shown to be both productive and hence, the turnover may be low. In panel D, the narrow entry channel of cycloox site (shown as a blue dumbbell-like structure) shows the narrow constriction leading to the cycloox cavity, wherein, AA adopts a very constrained binding modality that requires AA to squirm in like a snake entering a convoluted burrow. In panel E, the entire protein is shown as a transparent surface with the cycloox entry channel, AA, Y385 and heme of perox site aligned in a straight line. AA has to go in a linear fashion, adapt a L-like binding posture and then exit this narrow orifice as a hairpin like-structure, PGG2. The entry channel (highlighted in blue) constricts and then widens again into the cavity. In panel F, the narrow cycloox entry channel is shown with the other two channels which also may lead to cycloox cavity. Panel G shows the convoluted AA molecule and OH group of Y385 coloured red and the rest of the Y385 residue coloured in blue. Panel H shows the view from perox channel with other aligned entities (Y385, AA and the cycloox channel) behind the heme (red stick).*

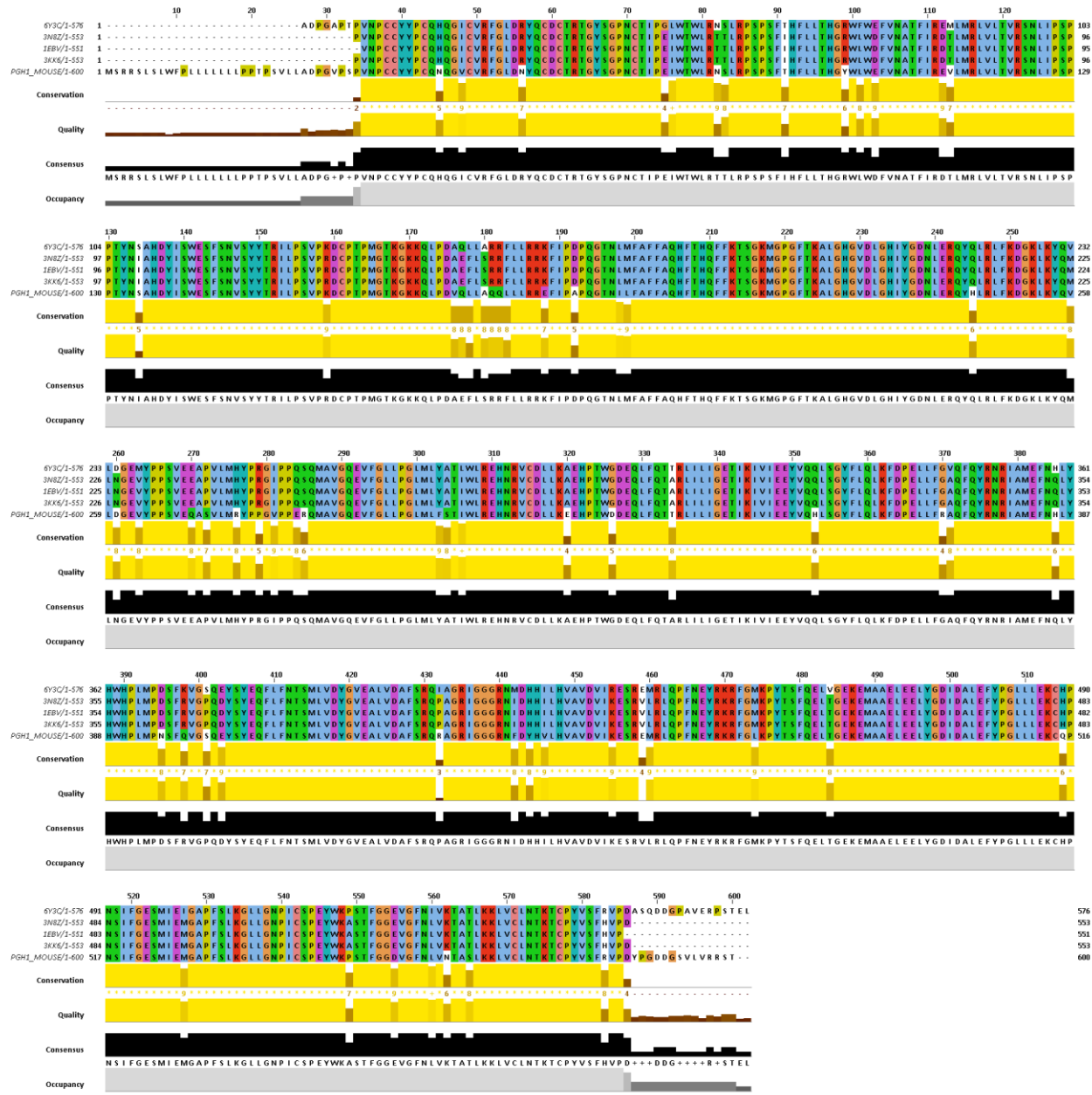


Figure S4. Comparison of *mCOX1* with *hCOX1* (*h6Y3C*) and sheep *COX1* (*3N8Z*, *1EBV* and *3KK6*) residues. Below this, conserved active site residues of these various *COX1* proteins have been compared.

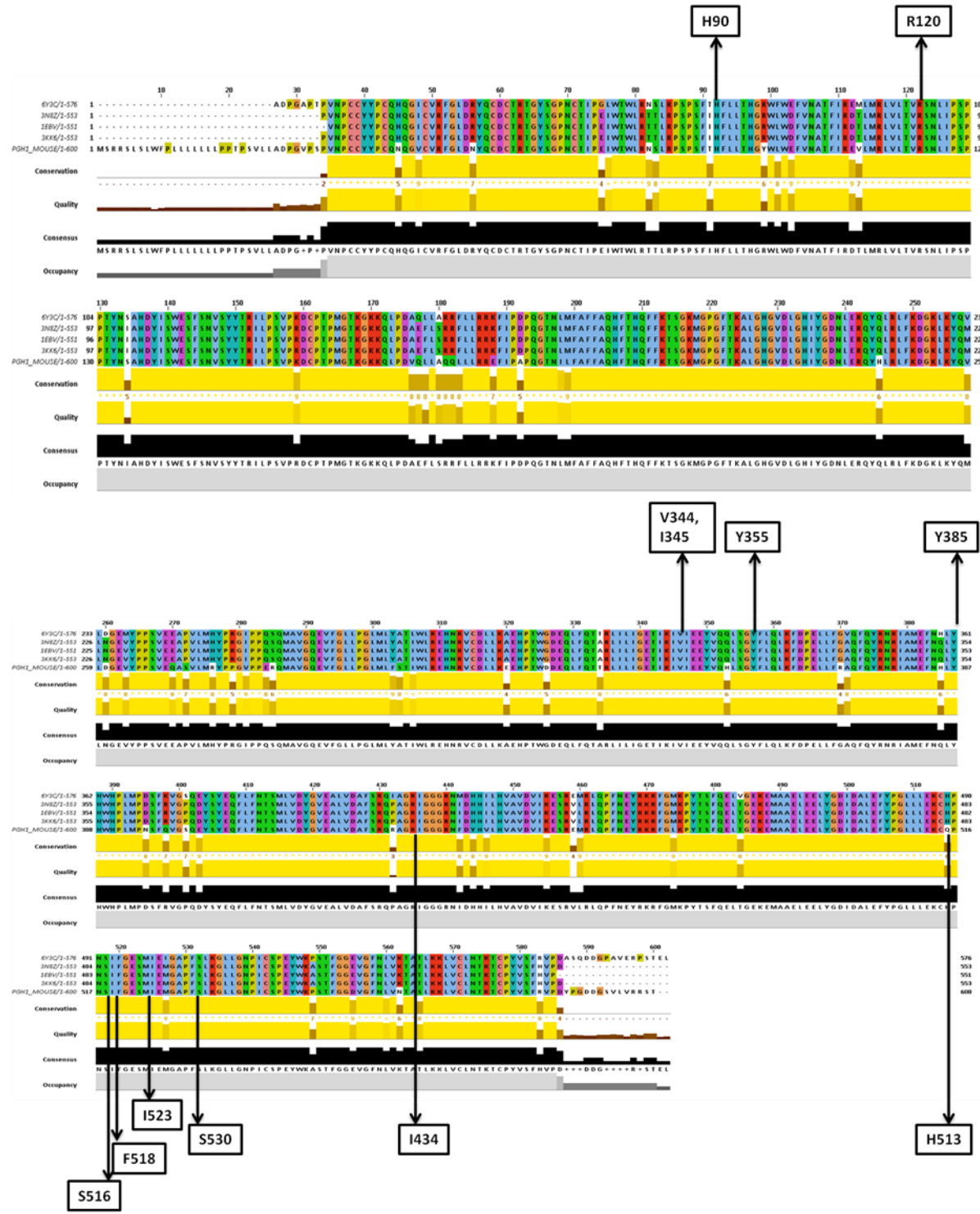


Figure S5. Active site residues of COX1: When compared, most of the mouse COX-1 residues are conserved in sheep as well as humans in these Clustal-aligned sequences. There is a +2 deviation from the actual number. No crystal structure of mCOX1 was found and hence, mCOX1 sequence from Uniprot (ID: P22437) was taken and the sequences from the crystal structures of all 3 sheep and 1 human COX1 were compared, keeping mCOX1 active site amino acid residues reported in literature as the reference. Overall, most (almost 100%) of the active site residues of the protein sequences compared herein are conserved and hence, this justifies docking of various inhibitors to different COX1

proteins. An inhibitor of human COX1 should also inhibit mouse and sheep COX1 without any discrepancy (going merely by the logic of residue conservation and active site binding-based activity).

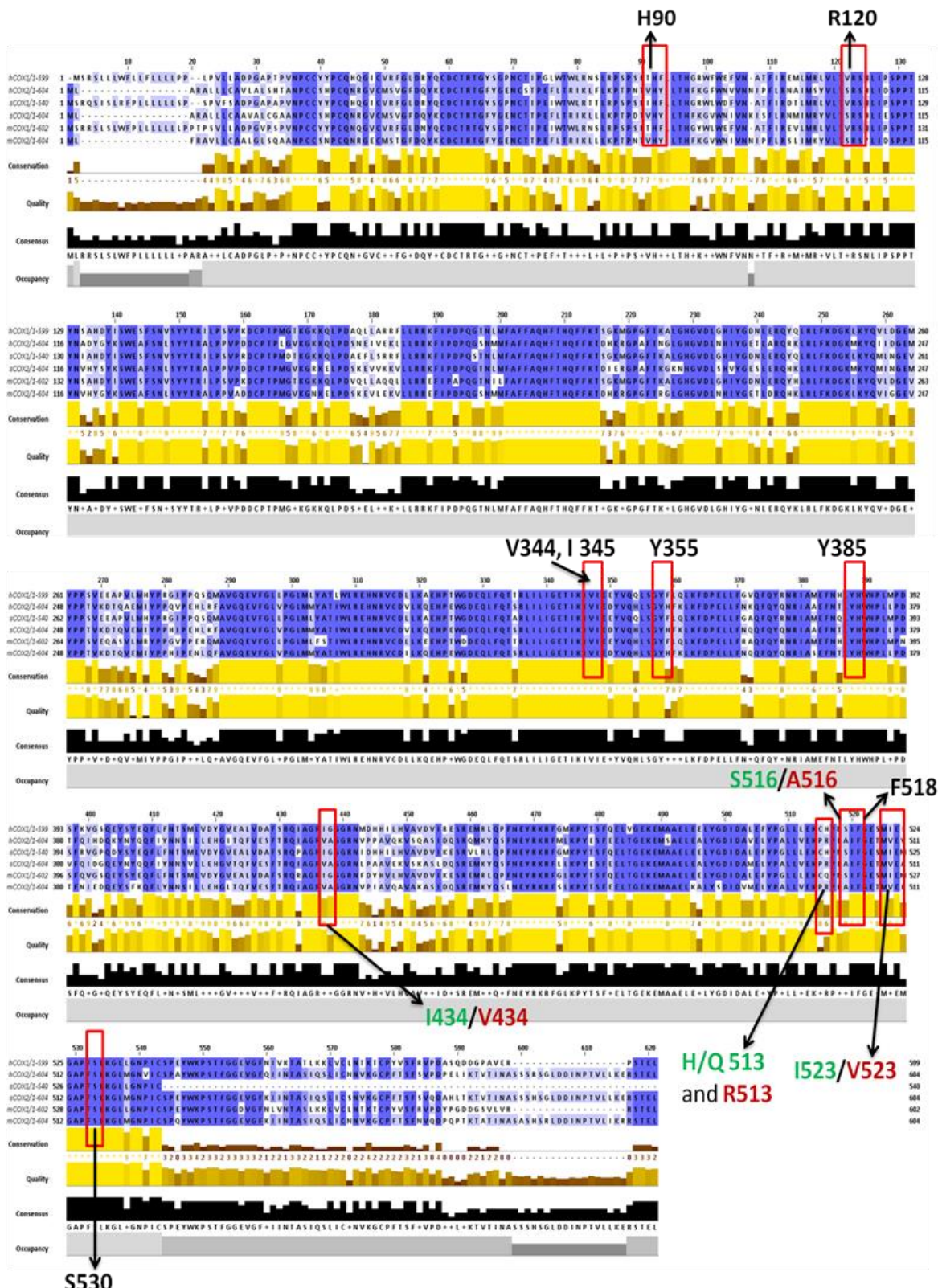


Figure S6. Sequence alignment of mammalian COX1 and COX2: When comparing the two key residues involved in COX action in the two COX isoforms (1 and 2) from different mammalian sources (human, sheep and mouse), the key active site residues in the cycloo cavity were mostly conserved. COX1 residues (unique to COX1) are coloured green and residues found in COX2 are coloured red. The residues which are common in both enzymes (conserved) are coloured black.

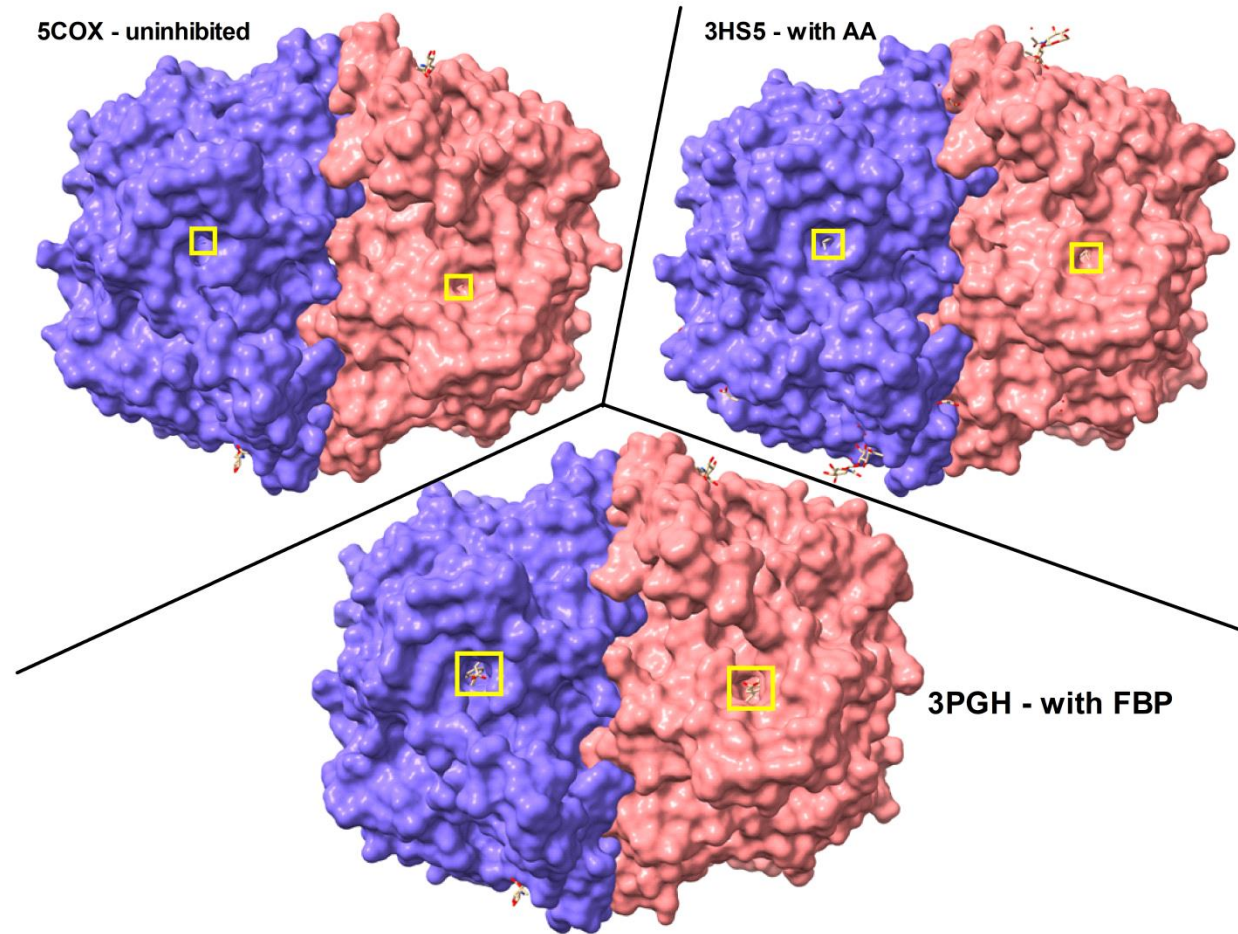


Figure S7. Closed active site channel (surface view) of mCOX2 (PDB ID: 5COX), mCOX2 bound with AA substrate (PDB ID: 3HS5) and mCOX2 with flurbiprofen, a cyclooxygenase inhibitor which is known to bind to the active site channel and thereby, preclude entry of substrate and product in and out of the cyclooxygenase active site. The dynamism of the active site entry channel (and lobby) is not exactly clear, but Comparison of the three dimeric structures of mCOX2 shows that the active site channel “opens up” to accommodate the substrates and inhibitors. However, the entire cyclooxygenase enzyme is presumed to be rigid, with minimal differences being observed between inhibited and uninhibited (or substrate-bound) structures.

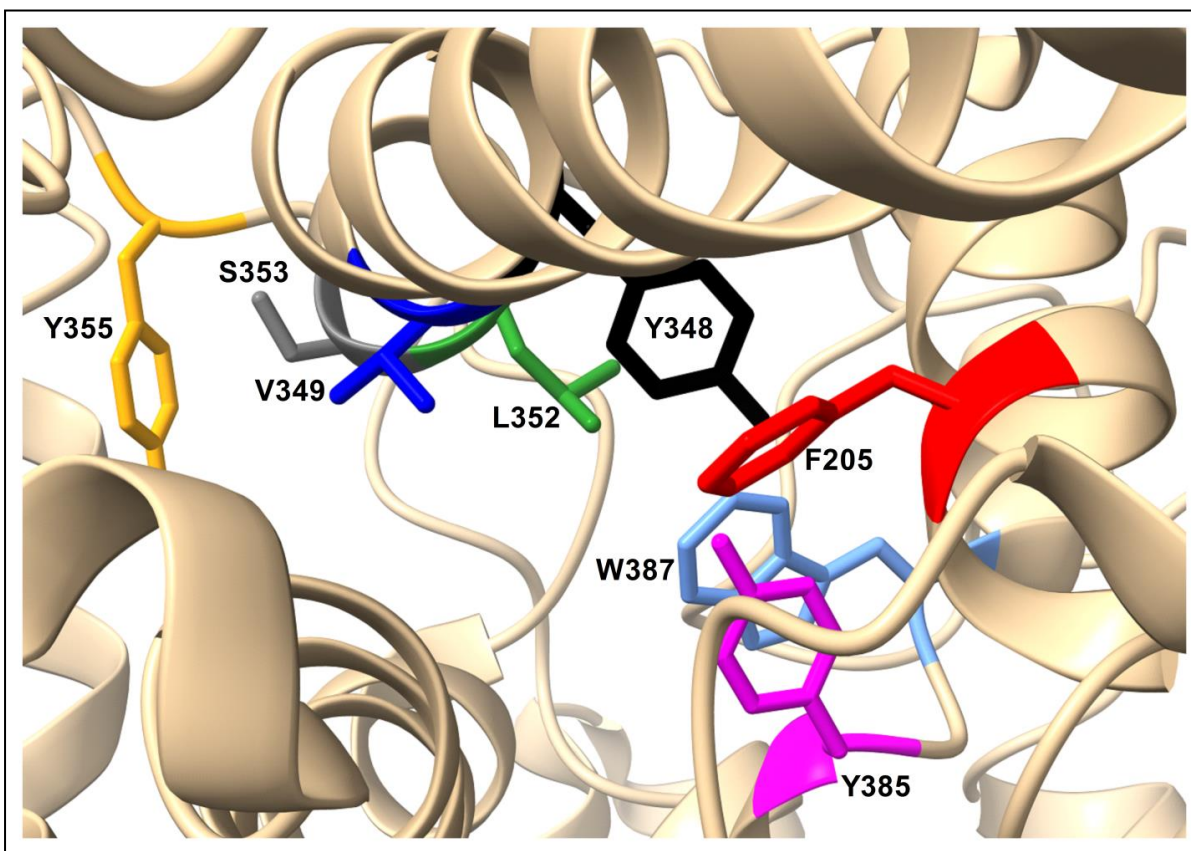


Figure S8. Positions of mutated residues in Malkowski et al. (2001) with respect to the catalytic Y385 residue.

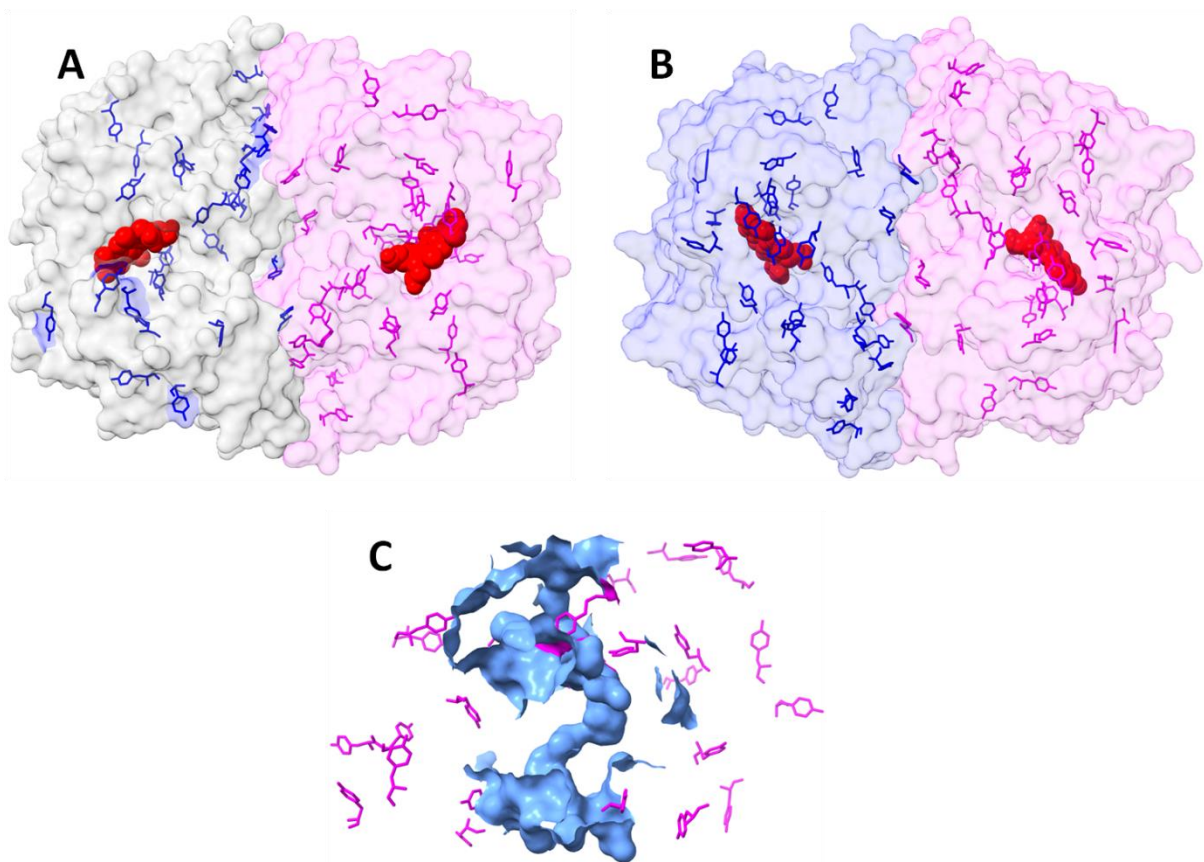


Figure S9: Presence of tyrosine residues in *mCOX2* (A) and *hCOX2* (B) dimers. Tyr residues in the two monomers are coloured demarcate them, and C. presence of tyrosine residues around the internal tunnel system in *hCOX1*. There are 27 tyrosine residues in cyclooxygenases

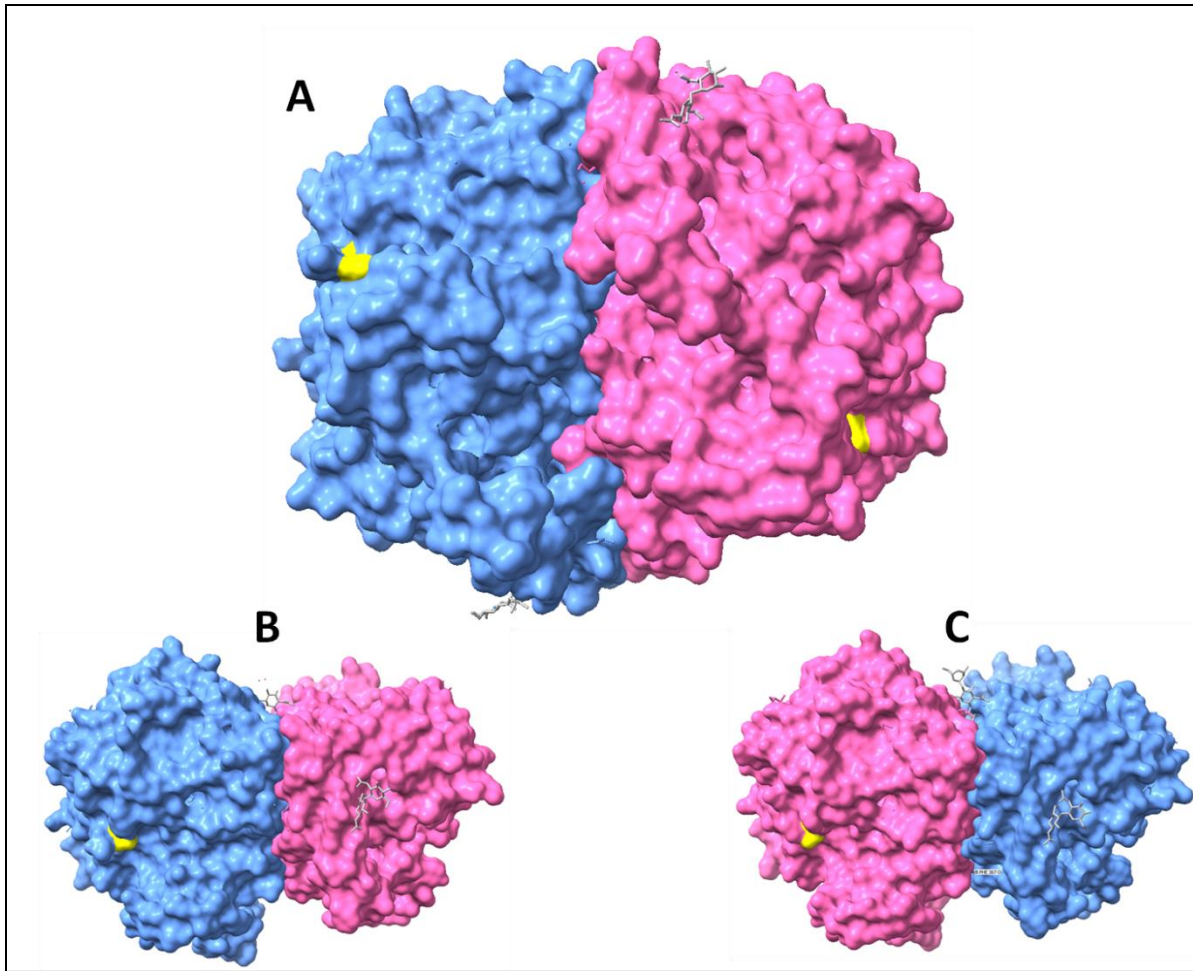


Figure S10. Location of N581 (yellow), whose mutation drastically altered COX enzyme activity. A – the position of the N581 residue in hCOX2 is marked as yellow in the surface view of the protein dimer. In panels B and C, the bottom side facing the membrane and the top side (perox cavity-ward) is shown. Here, the position of the N581 residue can be seen to be far away from the AA entry channel.

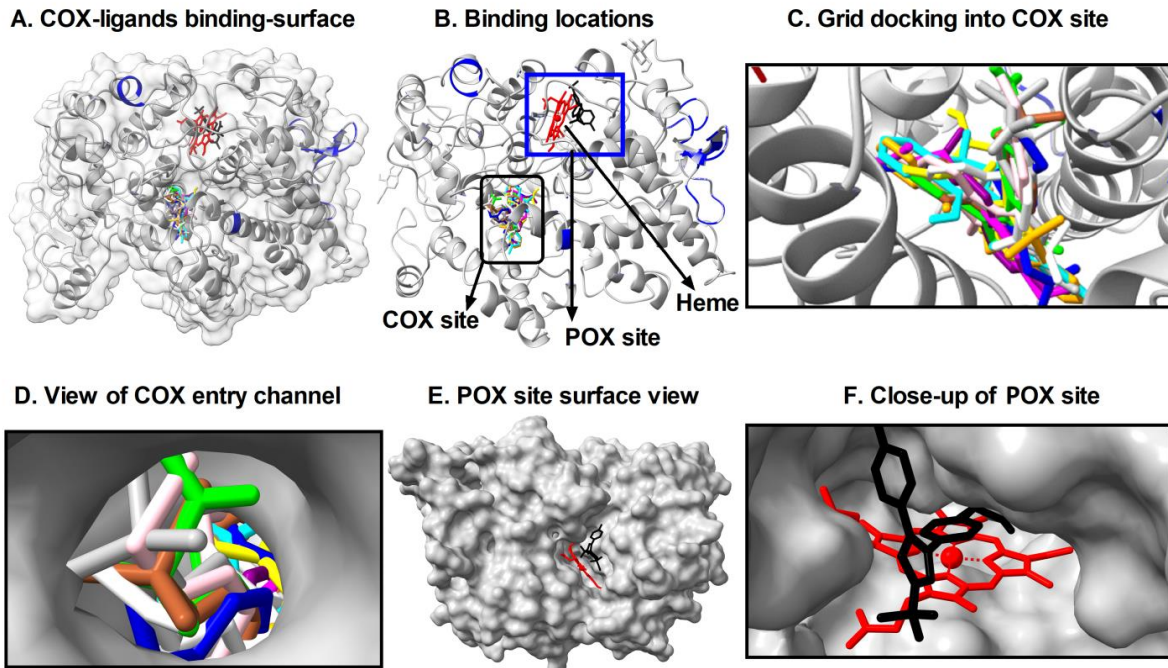


Figure S11: Visual representation of the docking data of inhibitors with cyclooxygenase-2. In panel A, an overview of the binding of the 11 inhibitors to PDB ID - 1CX2 from Table 3 is shown. In panel B, the binding locations of the 11 docked inhibitors (as given in Table 3) to mCOX2 (1CX2) is shown. Panel C shows the inhibitors coloured differently as sticks at the cycloxo binding site. In panel D, the entry channel of mCOX2 is shown with the inhibitors docking into the cavity. CXB, a coxib, was found to dock with greater affinity to the perox site, instead of the cycloxo site, which is shown in panels E and F. Colour codes for the docked inhibitors: CXB, black; VCB, lime green; RCB, brown; SDS, pink; PXM, orange; NMS, white; NPX, purple; NBM, magenta; MXM, cyan; IMC, dark blue and DCF, yellow.

Table S1. Physical properties of the various substrates/inhibitors that may affect mechanism

Inhibitors									
Name	No.of Rotatable Bonds	No.of H-Bond Acceptors	TPSA (Å ²)	Log P	Consensus Log P	Log S	Bioavailability Score	Mol.Wt (g/mol)	No.of H Bond Donors
CXB	4	7	86.36	2.56	3.40	-4.57	0.55	381.37	1
VXB	3	5	94.57	1.78	2.49	-3.81	0.55	314.36	1
RCB	3	4	68.82	2.13	2.79	-3.42	0.55	314.36	0
SDS	4	3	62.60	3.18	4.78	-5.09	0.85	340.41	1
PXM	3	5	107.98	1.67	1.38	-4.01	0.56	331.45	2
NBM	5	5	109.60	1.78	1.66	-3.48	0.55	308.31	1
NMS	3	3	46.53	1.92	2.76	-3.61	0.85	230.26	1
NPX	4	2	26.30	2.74	3.23	-3.37	0.55	228.29	0
MXM	3	5	136.22	1.74	1.73	-4.34	0.56	351.40	2
IMC	5	4	68.53	2.76	3.63	-4.86	0.85	357.79	1
DCF	4	2	49.33	1.98	3.66	-4.65	0.85	296.15	2
Substrates									
AA	14	1	37.30	6.22	-	-	0.54	304.47	1
PGG ₂	13	5	85.22	4.52	-	-	0.52	368.47	2
PGH ₂	12	4	75.99	4.02	-	-	0.67	352.47	2
PGI ₂	10	4	86.99	3.41	-	-	0.70	352.47	3
TXA ₂	12	4	75.99	3.82	-	-	0.72	352.47	2
LTC ₄ Negative control	25	7	216.35	2.78	-	-	0.62	625.78 6	8

Table S2: Grid-centered docking data of downstream product control molecules with various COX enzymes

Protein & Source	Ligands	Perox site		Cycloo site
		K _d (μM)	K _d (μM)	Cycloo site
COX1	3KK6 (sheep)	LTC ₄	-	14580
		TXA ₂	6.2	6.0
		PTC	0.3	2.1
	1EBV (sheep)	LTC ₄	-	4962
		TXA ₂	-	0.3
		PTC	-	0.1
	3N8Z (sheep)	LTC ₄	18520	3256
		TXA ₂	16.4	4.4

		PTC	4.2	13.0
6Y3C (human)	LTC ₄	15459	-	
	TXA ₂	2.2	3.2	
	PTC	0.8	1.0	
COX2	5KIR (human)	LTC ₄	6530	4962
		TXA ₂	6.8	0.3
		PTC	1.0	0.1
	5F1A (human)	LTC ₄	61.7	28779
		TXA ₂	0.2	5.0
		PTC	0.07	5.6
	1CX2 (mouse)	LTC ₄	5.4	3050
		TXA ₂	0.9	23.0
		PTC	0.5	1.1

Table S3. Pharmacokinetics

Inhibitors	GI Absorption	BBB Permeant	P-gp substrate	CYP1A2 Inhibitor	CYP2C19 Inhibitor	CYP2C9 Inhibitor	CYP2D6 Inhibitor	CYP3A4 Inhibitor	Log K _p (Skin Permeation)
CXB	High	No	No	Yes	No	Yes	No	No	-6.21cm/s
VXB	High	No	No	Yes	No	No	No	Yes	-6.36cm/s
RCB	High	Yes	No	Yes	Yes	Yes	No	No	-6.61cm/s
SDS	High	No	No	Yes	Yes	Yes	No	No	-4.96cm/s
PXM	High	No	No	No	No	Yes	No	No	-6.15cm/s
NBM	High	No	No	No	Yes	Yes	Yes	Yes	-6.33cm/s
NMS	High	Yes	No	No	No	No	No	No	-5.33cm/s
NPX	High	Yes	No	Yes	Yes	No	Yes	No	-5.51cm/s
MXM	High	No	No	No	No	Yes	No	Yes	-6.01cm/s
IMC	High	Yes	No	Yes	Yes	Yes	No	No	-5.45cm/s

Table S4. Amino acid interaction with the inhibitors (grid docking):

A. 1CX2, MOUSE COX2

Compounds	Conventional H-Bonds	Van der Waals	Pi-Sulfur/Pi-Cation/Pi-Anion	Pi-Sigma/amide Pi-stacked	C-H bond donor	Alkyl/Pi-alkyl	Halogen Bond
CXB	Q ₂₀₃ , H ₂₀₇	R ₂₂₂ , I ₂₇₄ , Q ₂₈₉ , L ₂₉₈ , V ₂₉₅	H ₂₁₄	V ₂₉₁	-	K ₂₁₁	-
VXB	H ₉₀ , L ₃₅₂ , R ₅₁₃	R ₁₂₀ , Q ₁₉₂ , S ₃₅₃ , L ₃₅₉ , Y ₃₈₅ , W ₃₈₇ , A ₅₁₆ , I ₅₁₇ , F ₅₁₈ , S ₅₃₀ , L ₅₃₁	-	V ₃₄₉ , V ₅₂₃ , A ₅₂₇	-	Y ₃₅₅	-
RCB	H ₉₀ , R ₁₃	R ₁₂₀ , Q ₁₉₂ , V ₃₄₉ , S ₃₅₃ , Y ₃₅₅ , W ₃₈₇ , A ₅₁₆ , I ₅₁₇ , F ₅₁₈ , G ₅₂₆ , S ₅₃₀	-	V ₅₂₃	-	L ₃₅₂ , A ₅₂₇	-
SDS	S ₅₃₀	Q ₁₉₂ , I ₃₄₅ , Y ₃₄₈ , Y ₃₅₅ , L ₃₈₄ , W ₃₈₇ , R ₅₁₃ , M ₅₂₂ , G ₅₂₆ , L ₅₃₄	H ₉₀	S ₃₅₃ , V ₅₂₃ , A ₅₂₇	-	V ₃₄₉ ,	-

						L ₃₅₂ , A ₅₁₆ , I ₅₁₇ , F ₅₁₈ , L ₅₃₁	
PXM	V ₅₂₃	M ₁₁₃ , L ₃₅₂ , Y ₃₅₅ , F ₃₈₁ , L ₃₈₄ , Y ₃₈₅ , W ₃₈₇ , F ₅₁₈ , G ₅₂₆ , S ₅₃₀	R ₁₂₀ , M ₁₂₂	-	S ₃₅₃	V ₁₁₆ , V ₃₄₉ , L ₃₅₉ , A ₅₂₇ , L ₅₃₁	-
NBM	R ₁₂₀	V ₁₁₆ , L ₃₅₂ , F ₃₈₁ , L ₃₈₄ , Y ₃₈₅ , W ₃₈₇ , F ₅₁₈ , M ₅₂₂ , V ₅₂₃ , S ₅₃₀	-	A ₅₂₇	G ₅₂₆	V ₃₄₉ , Y ₃₅₅ , L ₃₅₉ , L ₅₃₁	-
NMS	H ₉₀ , R ₅₁₃	H ₉₀ , V ₃₄₉ , L ₃₅₉ , A ₅₁₆ , F ₅₁₈ , M ₅₂₂ , G ₅₂₆ , S ₅₃₀	-	V ₅₂₃	-	L ₃₅₂ , A ₅₂₇	-
NPX	R ₁₂₀ , Y ₃₈₅ , S ₅₃₀	Y ₃₄₈ , L ₃₅₂ , Y ₃₅₅ , F ₃₈₁ , L ₃₈₄ , W ₃₈₇ , F ₅₁₈ , V ₅₂₃ , G ₅₂₆	-	V ₃₄₉ , A ₅₂₇	-	V ₁₁₆ , L ₃₅₉ , L ₅₃₁	-
MXM	Y ₃₅₅ , Y ₃₈₅ , V ₅₂₃	L ₉₃ , L ₃₅₂ , S ₃₅₃ , L ₃₈₄ , G ₅₂₆ , S ₅₃₀	R ₁₂₀ , Y ₃₄₈ , W ₃₈₇ , M ₅₂₂	F ₅₁₈	-	V ₁₁₆ , V ₃₄₉ , L ₃₅₉ , A ₅₂₇ , L ₅₃₁	-
IMC	-	V ₁₁₆ , L ₃₅₉ , R ₁₂₀ , R ₅₁₃ , G ₅₂₆ , S ₃₅₃ , A ₅₁₆ , S ₅₃₀ , Y ₃₅₅ , F ₅₁₈	-	V ₅₂₃ , W ₃₈₇	-	H ₉₀ , V ₃₄₉ , L ₃₅₂ , F ₃₈₁ , L ₃₈₄ , Y ₃₈₅ , A ₅₂₇ , L ₅₃₁	-
DCF	Y ₃₄₈ , Y ₃₈₅	R ₁₂₀ , S ₃₅₃ , Y ₃₅₅ , F ₃₈₁ , L ₃₈₄ , W ₃₈₇ , F ₅₁₈ , M ₅₂₂ , S ₅₃₀	-	G ₅₂₆	-	L ₃₅₂ , V ₅₂₃ , L ₅₃₁	-

B. 1EBV, SHEEP COX1

Compounds	Conventional H-Bonds	Van der Waals	Pi-Sulfur/Pi-Cation/Pi-Anion	Pi-Sigma/amide Pi-stacked	Carbon hydrogen bond donor	Alkyl/Pi-alkyl	Halogen Bond
CXB	R ₁₂₀ , Y ₃₈₅	V ₁₁₆ , T ₂₀₆ , F ₂₀₉ , V ₃₄₄ , Y ₃₄₈ , L ₃₅₂ , Y ₃₅₅ , L ₃₅₉ , I ₅₂₃ , F ₅₂₉ , L ₅₃₄ ,	F ₂₀₅ , F ₃₈₁ , M ₅₂₂	V ₃₄₉ , A ₅₂₇	S ₃₅₃	L ₃₈₄ , W ₃₈₇ , F ₅₁₈	-
VXB	N ₃₈₂	G ₂₀₃ , T ₂₀₆ , F ₂₁₀ , L ₂₉₅ , G ₃₈₃ , Y ₃₈₅ , W ₃₈₇ , I ₄₄₄	H ₂₀₇ , H ₃₈₆ , H ₃₈₈ , M ₃₉₁	A ₂₀₂	-	A ₁₉₉ , L ₃₉₀	-
RCB	L ₅₃₁	F ₂₀₉ , V ₃₄₄ , Y ₃₄₈ , S ₃₅₃ , F ₃₈₁ , L ₃₈₄ , Y ₃₈₅ , W ₃₈₇ , F ₅₁₈ , M ₅₂₂ , I ₅₂₃ , G ₅₂₆ , F ₅₂₉ , L ₅₃₄	F ₂₀₅	-	-	V ₃₄₉ , L ₃₅₂ , A ₅₂₇	-

SDS	-	Y ₃₄₈ , L ₃₅₂ , S ₃₅₃ , L ₃₈₄ , Y ₃₈₅ , I ₅₂₃ , F ₅₂₉ , G ₅₃₃ , L ₅₃₄	F ₂₀₅ , F ₃₈₁	G ₅₂₆	-	F ₂₀₉ , V ₃₄₉ , W ₃₈₇ , F ₅₁₈ , M ₃₂₂ , A ₅₂₇ , L ₅₃₁	-
PXM	L ₅₃₁	F ₂₀₅ , F ₂₀₉ , Y ₃₄₈ , V ₃₄₉ , L ₃₅₂ , L ₃₈₄ , Y ₃₈₅ , W ₃₈₇ , F ₅₁₈ , I ₅₂₃ , F ₅₂₉ , G ₅₃₃ ,	M ₅₂₂	F ₃₈₁ , G ₅₂₆	A ₅₂₇	L ₅₃₄	-
NBM	L ₅₃₁ , G ₅₃₃ , L ₅₃₄	F ₂₀₅ , F ₂₀₉ , V ₃₄₄ , Y ₃₄₈ , V ₃₄₉ , L ₃₅₂ , F ₃₈₁ , L ₃₈₄ , G ₅₂₆ , F ₅₂₉ , L ₅₃₂	-	Y ₃₈₅ , W ₃₈₇	-	F ₅₁₈ , M ₅₂₂ , I ₅₂₃	-
NMS	-	Y ₃₄₈ , L ₃₅₂ , S ₃₅₃ , F ₃₈₁ , F ₅₁₈ , M ₅₂₂ , I ₅₂₃ , G ₅₂₆ , F ₅₂₉ , L ₅₃₄	-	V ₃₄₉ , Y ₃₈₅ , W ₃₈₇	-	L ₃₈₄ , A ₅₂₇ , L ₅₃₁	-
NPX	F ₅₂₉ , L ₅₃₁ , L ₅₃₄	W ₃₄₈ L ₃₅₂ , Y ₃₈₅ , I ₅₂₃ G ₅₂₆ ,	M ₅₂₂	-	-	F ₂₀₅ , F ₂₀₉ , V ₃₄₉ , F ₃₈₁ , L ₃₈₄ , W ₃₈₇ , F ₅₁₈	-
MXM	L ₅₃₁	V ₃₄₉ , L ₃₅₂ , L ₃₈₄ , F ₅₁₈ , I ₅₂₃ , F ₅₂₉ , G ₅₃₃ ,	F ₂₀₅ , F ₃₈₁ , Y ₃₈₅ , M ₅₂₂	W ₃₈₇ , G ₅₂₆	A ₅₂₇	F ₂₀₉ , V ₂₂₈ , L ₅₃₄	-
IMC	-	F ₂₀₅ , V ₃₄₄ , I ₃₄₅ , Y ₃₄₈ , L ₃₅₂ , N ₃₇₅ , I ₃₇₇ , L ₃₈₄ , Y ₃₈₅ , W ₃₈₇ , G ₅₂₆ , F ₅₂₉ , G ₅₃₃ ,	-	F ₃₈₁	-	F ₂₀₉ , V ₃₄₉ , F ₅₁₈ , M ₅₂₂ , I ₅₂₃ , A ₅₂₇ , L ₅₃₁ , L ₅₃₄	-
DCF	A ₅₂₇	R ₁₂₀ , S ₃₅₃ , Y ₃₅₅ , F ₃₈₁ , L ₃₈₄ , W ₃₈₇ , M ₅₂₂ , F ₅₂₉ , L ₅₃₄	-	G ₅₂₆		V ₃₄₉ , L ₃₅₂ , F ₅₁₈ , I ₅₂₃	-

C. 3KK6, SHEEP COX1

Compounds	Conventional H-Bonds	Van der Waals	Pi-Sulfur/Pi-Cation/Pi-Anion	Pi-Sigma/amide Pi-stacked	Carbon hydrogen bond donor	Alkyl/Pi-alkyl	Halogen Bond
CXB	I ₅₁₇ , F ₅₁₈	R ₁₂₀ , Y ₃₅₅ , S ₅₁₆ , G ₅₂₆ , L ₅₃₁ , (Unfavourable Acceptors- Q ₁₉₂ , L ₃₅₂)	H ₉₀ ,	I ₅₂₃	S ₃₅₃	V ₁₁₆ , V ₃₄₉ , L ₃₅₉ , L ₃₈₄ , W ₃₈₇ , M ₅₂₂ , A ₅₂₇	-

VXB	Q ₁₉₂ , L ₃₅₂ , S ₃₅₃ , I ₅₁₇	G ₃₅₄ , L ₃₅₉ , W ₃₈₇ , S ₅₁₆ , M ₅₂₂ , S ₅₃₀ , L ₅₃₁	-	V ₃₄₉ , I ₅₂₃ , A ₅₂₇ , Y ₃₅₅ P ₅₁₈ , G ₅₂₆ ,	H ₉₀	-	-
RCB	I ₅₁₇	V ₃₄₉ , S ₃₅₃ , W ₃₈₇ , S ₅₁₆ , M ₅₂₂ , S ₅₃₀ , L ₅₃₁	H ₉₀	L ₃₅₂ , Y ₃₅₅ , F ₅₁₈ , I ₅₂₃ , G ₅₂₆ ,	-	A ₅₂₇	-
SDS	M ₅₂₂	H ₉₀ , R ₁₂₀ , S ₃₅₃ , W ₃₈₇ , F ₅₁₈ , M ₅₂₅ , G ₅₂₆ , S ₅₃₀ , L ₅₃₁	Y ₃₅₅	V ₁₁₆ , I ₅₂₃ , A ₅₂₇	-	L ₉₃ , V ₃₄₉ , L ₃₅₇ , L ₃₅₉	-
PXM	A ₅₂₇	R ₁₂₀ , L ₃₅₂ , Y ₃₅₅ , F ₃₈₁ , L ₃₈₄ , Y ₃₈₅ , W ₃₈₇ , F ₅₁₈ , G ₅₂₆ , S ₅₃₀	M ₅₂₂	V ₃₄₉	I ₅₂₃ , S ₃₅₃	V ₁₁₆ , L ₃₅₉ , L ₅₃₁	-
NBM	A ₁₂₀	V ₁₁₆ , V ₃₄₉ , S ₃₅₃ , Y ₃₅₅ , F ₃₈₁ , F ₅₁₈ , - S ₅₃₀ , L ₅₃₁	-	L ₃₅₂ , G ₅₂₆	-	L ₃₈₄ , Y ₃₈₅ , W ₃₈₇ , M ₅₂₂ , I ₅₂₃ , A ₅₂₇	-
NMS	R ₁₂₀ , E ₅₂₄	P ₈₄ , S ₈₅ , P ₈₆ , L ₁₁₅ , V ₁₁₉ , F ₄₇₀ , G ₄₇₁	-	L ₅₂₃	V ₁₁₆ ,	I ₈₉ , P ₅₂₈	-
NPX	R ₁₂₀	H ₉₀ , L ₉₃ , V ₁₁₆ , Y ₃₅₅ , S ₅₁₆	-	S ₃₅₃ , I ₅₂₃	Q ₁₉₂	V ₃₄₉ , L ₃₅₂ , I ₅₁₇ , F ₅₁₈ , A ₅₂₇ , L ₅₃₁	-
MXM	-	R ₁₂₀ , L ₃₅₂ , Y ₃₅₅ , F ₅₁₈ I ₅₂₃ , G ₅₂₆ , S ₅₃₀ , L ₅₃₁	M ₅₂₂	V ₁₁₆ , Y ₃₈₅	S ₃₅₃	V ₃₄₉ , L ₃₅₉ , F ₃₈₁ , L ₃₈₄ , W ₃₈₇ , A ₅₂₇	-
IMC	M ₅₂₂	L ₁₁₇ , R ₁₂₀ , Y ₃₅₅ , K ₃₆₀ , W ₃₈₇ , I ₅₁₇ , G ₅₂₆ , S ₅₃₀	M ₁₁₃	V ₃₄₉ , L ₃₅₉ , I ₅₂₃ , A ₅₂₇ , L ₅₃₁	L ₃₅₂ , S ₃₅₃	V ₁₁₆ , I ₃₄₅ , F ₅₁₈	-
DCF	R ₁₂₀ , Y ₃₅₅ , I ₅₂₃	H ₉₀ , V ₁₁₆ , Y ₃₄₈ , S ₃₅₃ , W ₃₈₇ , S ₅₃₀ , L ₅₃₁	-	L ₃₅₂ , G ₅₂₆	-	V ₃₄₉ , F ₅₁₈ , M ₅₂₂ , A ₅₂₇	-

D. 3N8Z, SHEEP COX1

Compounds	Conventional H-Bonds	Van der Waals	Pi-Sulfur/Pi-Cation/Pi-Anion	Pi-Sigma/amide Pi-stacked	Carbon hydrogen bond donor	Alkyl/Pi-alkyl	Halogen Bond
CXB	R ₁₂₀ , Q ₁₉₂ ,	G ₃₅₄ , L ₃₅₉ , S ₅₁₆ , I ₅₁₇ , G ₅₂₆ , S ₅₃₀	-	L ₃₅₂ , Y ₃₅₅	H ₉₀	V ₁₁₆ , V ₃₄₉ ,	-

	S_{353} , H_{513}					Y_{355} , L_{384} , W_{387} M_{522} , A_{527} , L_{531}	
VXB	-	$V_{116}, R_{120}, Y_{348}, S_{353}, Y_{355}, L_{384}, Y_{385}, M_{522}$	F_{381}, W_{387}	$L_{352}, I_{523}, G_{526}, A_{527}$	S_{530}	$V_{349}, F_{518}, L_{531}$	-
RCB	-	$Y_{355}, L_{359}, L_{384}, Y_{385}, F_{518}, M_{522}, S_{530}, L_{531}, L_{359}$	F_{381}, W_{387}	L_{352}, I_{523}	S_{353}	V_{349}, A_{527}	-
SDS	M_{522}	$R_{120}, L_{352}, S_{353}, L_{357}, L_{384}, W_{387}, F_{518}, G_{526}, S_{530}$	-	$V_{116}, V_{349}, I_{523}, A_{527}$	-	$L_{93}, Y_{355}, L_{359}, L_{531}$	-
PXM	R_{120}, S_{530}	$M_{113}, L_{352}, Y_{355}, F_{381}, Y_{385}, W_{387}, F_{518}, M_{522}, I_{523},$	-	V_{116}, G_{526}	S_{353}	$V_{349}, L_{359}, L_{384}, A_{527}, L_{531}$	-
NBM	R_{120}	$V_{116}, V_{349}, S_{353}, Y_{355}, F_{518}, M_{522}, G_{526}, S_{530}, L_{531},$	-	L_{352}, Y_{385}	-	$F_{381}, L_{384}, W_{387}, I_{523}, A_{527}$	-
NMS	R_{120}	$V_{116}, Y_{348}, S_{353}, L_{359}, F_{381}, Y_{385}, W_{387}, F_{518}, M_{522}, G_{526}, L_{531}$	Y_{355}, S_{530}	-	-	$V_{349}, L_{352}, I_{523}, A_{527}$	-
NPX	R_{120}, Y_{355}	$V_{116}, G_{526}, S_{530}$	-	L_{352}, I_{523}	-	$V_{349}, L_{359}, L_{384}, W_{387}, F_{518}, M_{522}, A_{527}, L_{531}$	-
MXM	A_{120}, S_{530}	$M_{113}, L_{352}, Y_{355}, F_{518}, M_{522}, I_{523}$	$W_{387},$	V_{116}, Y_{385}	S_{353}	$V_{349}, L_{359}, F_{381}, L_{384}, A_{527}, L_{531}$	-
IMC	R_{120}	$V_{116}, Y_{348}, F_{518}, M_{522}, G_{526}, S_{530}$	-	$V_{349}, Y_{385}, W_{387}, I_{523}, A_{527},$	$L_{93}, S_{353}, L_{359},$	$H_{90}, L_{352}, Y_{355}, F_{381}, L_{384}, L_{531}$	-
DCF	Y_{348}, Y_{385}	$V_{116}, R_{120}, S_{353}, F_{381}, L_{384}, W_{387}, M_{522}, G_{526}, S_{530}$	-	L_{352}, A_{527}	-	$V_{349}, Y_{355}, I_{523}, L_{531}$	

E. SF1A, HUMAN COX2

Compounds	Conventional H-Bonds	Van der Waals	Pi-Sulfur/Pi-Cation/Pi-Anion	Pi-Sigma/amide Pi-stacked	Carbon hydrogen bond donor	Alkyl/Pi-alkyl	Halogen Bond
CXB	H ₉₀ , R ₁₂₀ , Q ₁₉₂ , L ₃₅₂	M ₁₁₃ , A ₅₁₆ , I ₅₁₇ , M ₅₂₂ , G ₅₂₆ (Unfavourable Donor-Donor=F ₅₁₈)	-	V ₅₂₃ , A ₅₂₇	A ₅₁₃	V ₁₁₆ , V ₃₄₉ , Y ₃₅₅ , L ₃₅₉ , W ₃₈₇ , L ₅₃₁	-
VXB	-	T ₂₀₆ , F ₂₀₉ , V ₃₄₄ , Y ₃₄₈ , G ₅₂₆ , S ₅₃₀ , L ₅₃₄	F ₂₀₅ , F ₃₈₁ , Y ₃₈₅	V ₃₄₉ , L ₃₅₂ , A ₅₂₇	-	W ₃₈₇ , F ₅₁₈ , M ₅₂₂ , V ₅₂₃ , L ₅₃₁	-
RCB	-	F ₂₀₅ , V ₃₄₄ , Y ₃₄₈ , S ₃₅₃ , Y ₃₅₅ , L ₃₅₉ , F ₃₈₁ , L ₃₈₄ , Y ₃₈₅ , W ₃₈₇ , M ₅₂₂ , G ₅₂₆ , L ₅₃₁	-	L ₃₅₂ , A ₅₂₇	S ₅₃₀	V ₃₄₉ , V ₅₂₃	
SDS	R ₁₂₀ , Y ₃₅₅	H ₉₀ , L ₉₃ , V ₁₁₆ , Y ₃₄₈ , L ₃₅₉ , F ₃₈₁ , Y ₃₈₅ , G ₅₂₆ , S ₅₃₀	W ₃₈₇	V ₅₂₃ , A ₅₂₇	-	V ₃₄₉ , L ₃₅₂ , L ₃₈₄ , F ₅₁₈ , M ₅₂₂ , L ₅₃₁	S ₃₅₃
PXM	V ₅₂₃	R ₁₂₀ , Y ₃₄₈ , S ₃₅₃ , F ₃₈₁ , L ₃₈₄ , Y ₃₈₅ , W ₃₈₇	M ₅₂₂	Y ₃₅₅ , F ₅₁₈ , G ₅₂₆	-	V ₁₁₆ , V ₃₄₉ , L ₃₅₂ , L ₃₅₉ , A ₅₂₇ , L ₅₃₁	-
NBM	R ₁₂₀	V ₁₁₆ , S ₃₅₃ , Y ₃₅₅ , L ₃₅₉ , F ₅₁₈ , S ₅₃₀ , L ₅₃₁	M ₅₂₂	G ₅₂₆	-	V ₃₄₉ , F ₃₈₁ , L ₃₈₄ , Y ₃₈₅ , W ₃₈₇ ,	-
NMS	A ₁₂₀	V ₁₁₆ , V ₃₄₉ , L ₃₅₉ , W ₃₈₇ , F ₅₁₈ , M ₅₂₂ , G ₅₂₆ , S ₅₃₀ , L ₅₃₁	Y ₃₅₅	L ₃₅₂ , V ₅₂₃	S ₃₅₃	A ₅₂₇	-
NPX	R ₁₂₀ , Y ₃₅₅	F ₃₈₁ , L ₃₈₄ , M ₅₂₂ , S ₅₃₀	-	V ₃₄₉ , L ₃₅₂ , G ₅₂₆ , A ₅₂₇	-	V ₁₁₆ , L ₃₅₉ , Y ₃₈₅ , W ₃₈₇ , V ₅₂₃ , L ₅₃₁	-
MXM	R ₁₂₀	M ₁₁₃ , L ₃₅₂ , Y ₃₅₅ , S ₅₃₀	F ₃₈₁ , W ₃₈₇ , M ₅₂₂	Y ₃₈₅ , F ₅₁₈ , G ₅₂₆ , L ₅₃₁	S ₃₅₃ , V ₅₂₃	V ₁₁₆ , V ₃₄₉ , L ₃₅₉ , L ₃₈₄ , A ₅₂₇	-
IMC	R ₁₂₀ , Y ₃₅₅	L ₉₃ , V ₁₁₆ , S ₃₅₃ , L ₃₅₉ , R ₅₁₃ , M ₅₂₂ , G ₅₂₆ , S ₅₃₀ ,	-	V ₅₂₃ , A ₅₂₇	-	H ₉₀ , V ₃₄₉ , L ₃₅₂ , F ₃₈₁ , L ₃₈₄ , Y ₃₈₅ ,	-

						W_{387} , L_{531}	
DCF	-	R ₁₂₀ , F ₂₀₅ , S ₃₅₃ , Y ₃₅₅ , Y ₃₈₅ , W ₃₈₇ , M ₅₂₂ , S ₅₃₀ (Unfavourable Donor Donor-Y ₃₄₈)	-	L ₃₅₂ , A ₅₂₇	G ₅₂₆	V ₃₄₉ , V ₅₂₃ , L ₅₃₁	-

Table S5. Blind docking of COX inhibitors

		Binding Location	Binding Energy	Inhibitory Constant(μM)
1CX2, MOUSE COX2	CXB	All the ligands are bound to the cyclooxygenase site. But celecoxib is bound to the peroxisome site	-7.82	1.86
	VXB		-5.02	208.86
	RCB		-5.09	184.92
	SDS		-6.08	35.18
	PXM		-5.72	63.62
	NBM		-6.31	23.84
	NMS		-5.04	200.66
	NPX		-5.49	95.29
	MXM		-5.4	109.8
	IMC		-5.69	67.34
1EBV, SHEEP COX1	DCF		-5.56	84.38
	CXB	All the ligands are bound to the cyclooxygenase site. But Valdecoxib is bound to the peroxisome site	-6.96	7.97
	VXB		-7.56	2.9
	RCB		-7.34	4.16
	SDS		-7.33	4.26
	PXM		-7.13	5.96
	NBM		-8.64	4.66
	NMS		-7.31	4.38
	NPX		-7.18	5.46
	MXM		-8.27	8.61
3KK6, SHEEP COX1	IMC	Not checked	-7.14	5.84
	DCF		-7.0	7.37
	CXB			
	VXB			
	RCB			
	SDS			
	PXM			
	NBM			

	NMS		-7.07	6.6
	NPX		-7.58	2.77
	MXM		-8.54	0.551
	IMC		-6.69	12.44
	DCF		-5.45	0.101
3N8Z, SHEEP COX1	CXB		-7.16	5.63
	VXB		-9.85	0.060
	RCB		-9.21	0.177
	SDS		-7.06	6.7
	PXM		-7.39	3.8
	NBM		-7.73	2.17
	NMS		-7.43	3.59
	NPX		-7.91	-0.47
	MXM		-8.22	0.944
	IMC		-6.09	34.16
	DCF		-5.49	94.76
		Binding Location	Binding Energy	Inhibitory Constant(μM)
3KK6, SHEEP COX1	CXB	Not checked	-6.71	11.98
	VXB		-8.48	0.607
	RCB		-8.66	0.446
	SDS		-6.9	8.74
	PXM		-6.37	21.38
	NBM		-8.1	1.16
	NMS		-7.07	6.6
	NPX		-7.58	2.77
	MXM		-8.54	0.551
	IMC		-6.69	12.44
	DCF		-5.45	0.101
	CXB		-7.16	5.63
3N8Z, SHEEP COX1	VXB		-9.85	0.060
	RCB		-9.21	0.177
	SDS		-7.06	6.7
	PXM		-7.39	3.8
	NBM		-7.73	2.17
	NMS		-7.43	3.59
	NPX		-7.91	-0.47
	MXM		-8.22	0.944
	IMC		-6.09	34.16

	DCF		-5.49	94.76
5F1A, HUMAN COX2		Binding Location	Binding Energy	Inhibitory Constant(μM)
	CXB	Not checked		
	VXB		-7.02	7.12
	RCB		-7.23	5.01
	SDS		-7.01	7.32
	PXM		-7.88	1.68
	NBM		-6.72	11.88
	NMS		-6.09	34.1
	NPX		-6.12	32.54
	MXM		-3.92	1340
	IMC		-6.22	27.64
	DCF		-4.78	315.89
5KIR, HUMAN COX2	CXB	Not checked	-10.05	43.07
	VXB		-10.18	34.57
	RCB		-8.29	0.838
	SDS		-7.07	6.53
	PXM		-5.87	50.11
	NBM		-8.37	0.738
	NMS		-6.97	7.82
	NPX		-8.16	1.04
	MXM		-7.81	1.9
	IMC		-7.85	1.76
	DCF		-6.92	8.47

Table S6. COX1/COX2 specificity ratios (selectivity index) of the inhibitors from this study with references

Ligand	Selectivity index (COX1 IC ₅₀ /COX2 IC ₅₀ ratio)	Reference (selectivity index)	Comment from docking result (this work)
--------	--	-------------------------------	---

CCB	32 and 294	El-Dershaby et al., 2022; Patrignani et al., 2008	K_i values of inhibitors for COX1 either close to or much lower than for COX2 – it should be the other way around!
RCB	38 and 255	Patrignani et al., 2008; Vardeny and Solomon, 2008	ditto
VCB	28 and 61	Patrignani et al., 2008; Vardeny and Solomon, 2008	ditto
NMS	5.26	Rao and Knaus, 2008	ditto
MXM	13.8	Patrignani et al., 2008	ditto
NBM	Not found	Not found	-
DCF	4.52 and 24.4	El-Dershaby et al., 2022; Patrignani et al., 2008	ditto
SDS	0.03	Giuliano and Warner, 1999	K_i ratios (COX1/COX2) of inhibitors along expected lines (showing COX1 binding preference), but significant differences in the inhibition constant between COX1 proteins
PXC	3.1	Giuliano and Warner, 1999	ditto
IMC	0.21	El-Dershaby et al., 2022	ditto
NPX	0.49	Patrignani et al., 2008	Except for ICX2, the K_i values do not differ much between COX1 and COX2

Details of abbreviations used:

Bold and yellow highlight – COX2 specific/preferential drugs

Not bold, Green shading – COX1-preferential drugs

Bold italic Green shading – COX1-specific drug

Not bold, pink shading – non-selective (inhibits both)

Keeping 100 μM as a cut-off value for discriminating as good vs. poor binders, the combinations of receptor-ligand with poor predicted K_i values are shaded in red. Turquoise highlights depict discordances in preferential binding to either COX1 or COX2 (that is not expected, based on the category of the drug selected).

Supplementary references

El-Dershaby, N. H., El-Hawash, S. A., Kassab, S. E., Daabees, H. G., Abdel Moneim, A. E., & El-Miligy, M. M. (2022). Rational design and synthesis of new selective COX-2 inhibitors with In Vivo PGE2-lowering activity by tethering benzenesulfonamide and 1, 2, 3-triazole pharmacophores to some NSAIDs. *Pharmaceuticals*, 15(10), 1165.

Patrignani, P., Capone, M. L., & Tacconelli, S. (2008). NSAIDs and cardiovascular disease. *Heart*, 94(4), 395-397.

Vardeny, O., & Solomon, S. D. (2008). Cyclooxygenase-2 inhibitors, nonsteroidal anti-inflammatory drugs, and cardiovascular risk. *Cardiology clinics*, 26(4), 589-601.

Rao, P., & Knaus, E. E. (2008). Evolution of nonsteroidal anti-inflammatory drugs (NSAIDs): cyclooxygenase (COX) inhibition and beyond. *Journal of pharmacy & pharmaceutical sciences*, 11(2), 81s-110s.

Giuliano, F., & Warner, T. D. (1999). Ex vivo assay to determine the cyclooxygenase selectivity of non-steroidal anti-inflammatory drugs. *British journal of pharmacology*, 126(8), 1824-1830.